



# Toxicity Going Nano: Ionic Versus Engineered Cu Nanoparticles Impacts on the Physiological Fitness of the Model Diatom *Phaeodactylum tricornutum*

Marco Franzitta<sup>1,2\*</sup>, Eduardo Feijão<sup>1,3</sup>, Maria Teresa Cabrita<sup>4</sup>, Carla Gameiro<sup>1,4</sup>, Ana Rita Matos<sup>3,5</sup>, João Carlos Marques<sup>6</sup>, Johannes W. Goessling<sup>7</sup>, Patrick Reis-Santos<sup>1,8</sup>, Vanessa F. Fonseca<sup>1,9</sup>, Carlo Pretti<sup>2</sup>, Isabel Caçador<sup>1,5</sup> and Bernardo Duarte<sup>1,5</sup>

<sup>1</sup> MARE – Marine and Environmental Sciences Centre, Faculdade de Ciências da Universidade de Lisboa, Lisbon, Portugal,

<sup>2</sup> Department of Veterinary Sciences, University of Pisa, Pisa, Italy, <sup>3</sup> BioISI – Biosystems and Integrative Sciences Institute, Plant Functional Genomics Group, Departamento de Biologia Vegetal, Faculdade de Ciências da Universidade de Lisboa, Lisbon, Portugal, <sup>4</sup> Instituto do Mar e da Atmosfera, Lisbon, Portugal, <sup>5</sup> Departamento de Biologia Vegetal, Faculdade de Ciências da Universidade de Lisboa, Lisbon, Portugal, <sup>6</sup> MARE – Marine and Environmental Sciences Centre, c/o Department of Zoology, Faculty of Sciences and Technology, University of Coimbra, Coimbra, Portugal, <sup>7</sup> International Iberian Nanotechnology Laboratory, Braga, Portugal, <sup>8</sup> Southern Seas Ecology Laboratories, School of Biological Sciences, The University of Adelaide, Adelaide, SA, Australia, <sup>9</sup> Departamento de Biologia Animal, Faculdade de Ciências da Universidade de Lisboa, Lisbon, Portugal

## OPEN ACCESS

### Edited by:

Naser A. Anjum,  
Aligarh Muslim University, India

### Reviewed by:

Ilaria Corsi,  
University of Siena, Italy  
Tore Brembu,  
Norwegian University of Science  
and Technology, Norway

### \*Correspondence:

Marco Franzitta  
franzitta.marco@gmail.com

### Specialty section:

This article was submitted to  
Marine Pollution,  
a section of the journal  
Frontiers in Marine Science

**Received:** 02 March 2020

**Accepted:** 04 December 2020

**Published:** 22 December 2020

### Citation:

Franzitta M, Feijão E, Cabrita MT, Gameiro C, Matos AR, Marques JC, Goessling JW, Reis-Santos P, Fonseca VF, Pretti C, Caçador I and Duarte B (2020) Toxicity Going Nano: Ionic Versus Engineered Cu Nanoparticles Impacts on the Physiological Fitness of the Model Diatom *Phaeodactylum tricornutum*. *Front. Mar. Sci.* 7:539827. doi: 10.3389/fmars.2020.539827

Increasing input of Metal Engineered Nano Particles (MeENPs) in marine ecosystems has raised concerns about their potential toxicity on phytoplankton. Given the lack of knowledge on MeENPs impact on these important primary producers, the effects of Copper Oxide (CuO) ENPs on growth, physiology, pigment profiles, fatty acid (FA) metabolism, and oxidative stress were investigated in the model diatom *Phaeodactylum tricornutum*, to provide suitable biomarkers of CuO ENP exposure versus its ionic counterpart. Diatom growth was inhibited by CuO ENPs but not Ionic Cu, suggesting CuO ENP cytotoxicity. Pulse Modulated Amplitude (PAM) phenotyping evidenced a decrease in the electron transport energy flux, pointing to a reduction in chemical energy generation following CuO ENPs exposure, as well as an increase in the content of the non-functional Cu-substituted chlorophyll a (CuChl a). A significant decrease in eicosapentaenoic acid (C20:5) associated with a significant rise in thylakoid membranes FAs reflected the activation of counteractive measures to photosynthetic impairment. Significant increase in the omega 6/omega 3 ratio, underline expectable negative repercussions to marine food webs. Increased thiobarbituric acid reactive substances reflected heightened oxidative stress by CuO ENP. Enhanced Glutathione Reductase and Ascorbate Peroxidase activity were also more evident for CuO ENPs than ionic Cu. Overall, observed molecular changes highlighted a battery of possible suitable biomarkers to efficiently determine the harmful effects of CuO ENPs. The results suggest that the occurrence and contamination of these new forms of metal contaminants can

impose added stress to the marine diatom community, which could have significant impacts on marine ecosystems, namely through a reduction of the primary productivity, oxygen production and omega 6 production, all essential to sustain heterotrophic marine life.

**Keywords:** CuO nanoparticles, photobiology, oxidative stress, lipid metabolism, phytoplankton, cytotoxicity, marine systems

## INTRODUCTION

Trace metal pollution poses a serious threat to marine environments. Poor management of anthropogenic waste and the accumulation of trace metals in sediments and seawater can lead to detrimental alterations in metabolic pathways of marine organisms, as well as in entire coastal ecosystems (Prosi, 1981; Pan and Wang, 2012). A large part of metal pollution affects marine life through direct toxic effects of metal elements (e.g., Pb, Cd, and Hg), or by altering the equilibrium of essential trace metals (e.g., Fe, Cu, and Zn), which can become toxic at high concentrations (Sunda, 1989; Ansari et al., 2004; Wei et al., 2014). Considering that higher human population densities and associated anthropogenic activities generally occur near estuarine and coastal areas, these regions are among the most immediately affected ecosystems by human-generated waste (UNEP, 2006). Metals are typical contaminants, often emerging from local or upstream industries (Duarte et al., 2010; Cabrita et al., 2014; Duarte et al., 2017). Nowadays, new anthropogenic metal forms occur in marine environments as a consequence of increasing use of nanoparticles in a variety of industrial application (UNEP, 2006).

Although metal nanoparticles can arise from both natural (aquatic colloids, volcanic activity, and atmospheric dust) and anthropogenic (industrial emissions) sources (Nowack and Bucheli, 2007), and organisms have always been exposed to them (Klaine et al., 2008), Metal Engineered Nano Particles (MeENPs) should be considered and investigated separately (Oberdörster et al., 2005). The increasing use of MeENPs is raising concerns related to their potential role as new or emerging contaminants in marine ecosystems. Copper nanoparticles, as conductive material, have many applications such as catalyst and solid lubricant, in optical and electronic applications, in particular medical applications, in manufacturing of nanofluids, conductive films, and as antimicrobial agents (Din and Rehan, 2017; Zhang et al., 2018). The increasing interest in this type of nanoparticles at the industrial and commercial level is reflected by their escalating values from 2016 (10.92 Billion USD) to projected values of 25.26 Billion USD by 2022 (Research And Markets.com., 2018). Besides the current level of exposure of organisms, the increasingly widespread use of different types of MeENPs, and the predicted exponential increase in production volumes (Royal Commission on Environmental Pollution., 2008), will undoubtedly lead to greater impact over biota within all environmental compartments (Rip et al., 1995).

In principal, copper is an essential nutrient for microalgae at trace concentrations. It is component of several proteins and enzymes (e.g., plastocyanin, cytochrome oxidase, ascorbate

oxidase, and Cu/Zn superoxide dismutase) and involved in a variety of metabolic pathways (Twining and Baines, 2013). However, in excess presence, copper interferes with numerous physiological, biochemical, and structural processes inducing high toxicity in cells (Fernandes and Henriques, 1991; Hook et al., 2014). Previous studies reported microalgal growth inhibition (Cid et al., 1995), production of reactive oxygen species (ROS) and altered fatty acid (FA) production (Morelli and Scarano, 2004) in Cu-exposed microalgae. However, knowledge of the effects of MeENPs in microalgae as important primary producers of marine environments is limited.

Using variable fluorescence signals of chlorophyll *a* (Chl *a*) from photosystem II as a proxy, pulse modulated amplitude (PAM) represents a fast, non-invasive, quantitative and qualitative methodology to evaluate the photonic energy harvest and its transformation processes into electronic energy (Kumar et al., 2014). FAs that compose the lipidic fraction of membranes of phytoplankton organisms are widely used as biomarkers to evaluate exposure of multiple abiotic and biotic stressors including contaminants (Feijão et al., 2018; Duarte et al., 2019). FA profiles, depicting levels of linolenic acid 18:2 (omega-6), linoleic acid C18:3 and omega-3 FAs, such as the long-chain polyunsaturated (LC-PUFAs), eicosapentaenoic acid (EPA), and docosahexaenoic acid (DHA), are not only important structural elements controlling the cell metabolism (Fan et al., 2007), but are also of ecological importance due to their essential character for higher trophic levels (Arts et al., 2001; Parrish, 2009). The n-3 LC-PUFA originates from phytoplankton and its biomagnification through the food web is fundamental to sustain marine ecosystems (Saito and Aono, 2014). A decrease in the synthesis of these key biomolecules can have dangerous cascading effects on entire marine food webs (Gladyshev et al., 2013). Therefore, it is worth investigating if FAs have the potential to be efficient biomarkers of nanoparticle stress, as found for other stressors in marine organisms (Filimonova et al., 2016; Feijão et al., 2018).

The present work expands on the work done by Zhu et al. (2017), by providing an integrative and comprehensive approach to assess the effects of Copper Oxide (CuO) ENP on diatom physiology. It examines the photosynthetic metabolic pathway, the oxidative stress responses, the variations in lipid metabolism and the production of Cu substituted chlorophylls in the marine diatom *P. tricornutum*. This species is a cosmopolitan marine pennate diatom and is a common model organisms to study the effects of pollutant exposure due to its rapid response to trace element changes in the environment (Chen et al., 2012; Cabrita et al., 2018, 2016, 2013, 2014; Feijão et al., 2018). In order to evaluate the effects of Cu forms in *P. tricornutum*,

non-lethal concentrations of Cu were chosen in this study, similar to those found in previous analysis focusing on estuarine systems (Cabrita et al., 2018). Reported concentrations were assumed for both, dissolved and ENP forms, in order to compare effects at similar concentrations.

## MATERIALS AND METHODS

### Experimental Setup

*Phaeodactylum tricornutum* Bohlin (Bacillariophyceae; strain IO 108-01, IPMA) axenic cell cultures (maintained under asexual reproduction conditions) were grown in 250 ml of *f/2* medium (Guillard and Ryther, 1962), under controlled conditions for 6 days ( $18 \pm 1^\circ\text{C}$ , constant aeration and a 12 h light to 12 h dark photoperiod). The growth chamber was programmed with a sinusoidal function simulating sunrise and sunset, with light intensity at noon to simulate a natural light environment [RGB 1:1:1 (molar proportion), maximum photon flux density (PAR)  $80 \mu\text{mol photons m}^{-2} \text{s}^{-1}$ , 14/10 h day/night rhythm]. Initial cell concentration was approximately  $2.7 \times 10^5 \text{ cells mL}^{-1}$ , following the Organization for Economic Cooperation and Development (OECD) guidelines for algae bioassays (OECD, 2011). Cultures were exposed to increasing concentrations of copper in either ionic or ENP forms, namely 1 (low), 5 (medium), and 10 (high)  $\mu\text{g L}^{-1}$ , applied during the exponential growth phase (3 days after inoculation under the described conditions). Exposure trial occurred for an additional 3 days period. The ionic Cu form was  $\text{CuSO}_4$ , whilst Cu ENPs were purchased as CuO nanoparticles with a particle size less than 50 nm and a surface area of  $29 \text{ m}^2 \text{ g}^{-1}$  (Sigma-Aldrich, Catalog number 544868) These concentrations are in accordance with the observed concentrations in estuarine and coastal systems, considering total metal concentration, and were tested in the past, using the ionic Cu form and the same model diatom species (Duarte et al., 2014; Cabrita et al., 2016, 2018). For every metal concentration, 3 replicates were tested and compared to 3 control experiments without Cu treatment. All glassware were cleaned with  $\text{HNO}_3$  (20%) for 2 days, rinsed thoroughly with Milli-Q water ( $18.2 \text{ M}\Omega \text{ cm}$ ), and autoclaved to avoid contamination. Culture manipulations were performed under laminar airflow in sterile conditions. Samples were collected at the end of the 6th day of the experiment (after 3 days of exposure to the Cu forms), for cell counting, PAM measurements, determination of fresh weight and for biochemical analyses. After centrifuging the samples at  $6,000 \times g$  for 15 min at  $4^\circ\text{C}$ , the supernatant was removed and pellets were immediately frozen in liquid nitrogen and stored at  $-80^\circ\text{C}$  for biochemical analyses. Three replicates for each analysis were used for all treatments (control, ionic Cu- and CuO ENP-exposed cells).

### Cell Growth Rates

Cell counting of *P. tricornutum* was performed on a Neubauer improved counting chamber, under an Olympus BX50 (Tokyo, Japan) inverted microscope, at  $400\times$  magnification. Growth rates, estimated as the mean specific growth rate per day, were calculated from the difference between initial and final

logarithmic cell densities divided by the exposure period (Santos-Ballardo et al., 2015).

### Copper Cell Content

All labware for metal analysis were previously decontaminated in a nitric acid bath. Diatom pellets for metal analysis were processed according to Cabrita et al. (2014). Briefly, diatom pellets were double-washed with *f/2* medium to remove externally adsorbed copper ions. After washing, pellets were dried at  $60^\circ\text{C}$  until constant weight and mineralized in a Teflon reactor with  $\text{HNO}_3:\text{HClO}_4$  acid mixture (7:1) for 3 h at  $110^\circ\text{C}$ . After cooling, digestion products were added with ICP-grade Gallium as an internal standard ( $1 \text{ mg L}^{-1}$  final concentration). A  $5 \mu\text{L}$  aliquot of each sample digestion product was then transferred to silicon-coated quartz disks and evaporated to dryness at  $80^\circ\text{C}$ . Samples on quartz disks were analyzed by total X-ray fluorescence spectroscopy (TXRF) using a S2 PICOFOX (Bruker, Germany), featuring an air-cooled low power X-ray metal-ceramic tube with a molybdenum target, working at 50 W of max power, and a liquid nitrogen-free Silicon Drift Detector (SSD; Bruker, 2007). Each sample was irradiated for 1,000 s. Possible drift in the spectroscopic amplification was compensated or reset through gain correction (Bruker, 2007). The relative abundance of intensities of the different elements was processed by referring to the Gallium peak (internal standard). The interpretation of the TXRF spectra and Cu concentration calculations was performed using the software program SPECTRA 6.3 (Bruker AXS Microanalysis GmbH). To evaluate the potential release of copper from the nanoparticle form, a set of twin experiments was prepared with *f/2* medium and the nanoparticles in the same concentrations and experimental conditions as the exposure trials. Water samples from this trial were collected at the same timepoints as the exposure trial. Samples were centrifuged, to avoid nanoparticle contamination, and Gallium was added to the supernatant as internal standard and the samples analyzed by TXRF, according to the methodology described above for the cell Cu content analysis in this manuscript.

### Copper ENPs Characterization

Cu ENPs, dissolved in distilled water in a final concentration of  $40 \text{ mg L}^{-1}$ , were sonicated for 30 min, prior to dropcasting on 40 nm gold sputtered silicon substrates. Samples were air dried and then mounted on microscope stubs and grounded with Electrodag silver paint and copper tape. A dual-beam focused ion beam scanning electron microscope (SEM; FEI, Oregon, United States) was used to record Cu ENPs. Particle zeta potential was determined in experimental concentrations of Cu ENPs dissolved in *f/2* medium at the Nanophotonics & Bioimaging Facility of the International Iberian Nanotechnology Laboratory (Braga, Portugal), using a Dynamic Light Scattering System (DLSS; model SZ-100Z, Horiba Seisakusho, Japan). Cu ENP size distribution was surveyed using DLSS and through SEM (Supplementary Figures 1A–D). Particle elemental composition and X-ray fluorescence spectra was obtained from the Cu ENPs in *f/2* medium using by TXRF as abovementioned (S2 PICOFOX, Bruker, Germany; Supplementary Figure 1E).

## Chlorophyll a PAM Fluorometry

Pulse Modulated Amplitude chlorophyll fluorescence measurements were performed using a FluoroPen FP100 (Photo System Instruments, Czech) on samples in a 1 ml cuvette. Cell density was assessed daily using a non-actinic light to induce minimum fluorescence over time ( $F_t$ ). All fluorometric analyses were carried out in dark-adapted samples. Analysis of chlorophyll transient light curves was carried out with the OJIP test, which can be divided into four main steps. Level O represents all the open reaction centers (RCs) at the onset of illumination without reduction of primary plastoquinone pool (quinone A,  $Q_A$ ; fluorescence intensity lasts for 10 ms). The rise of fluorescence transient from O to J indicates the net photochemical reduction of  $Q_A$  (the stable primary electron acceptor of PS II) to  $Q_A^-$  (lasts for 2 ms). The transient phase from J to I is due to all reduced states of closed RCs such as  $Q_A^- Q_B^-$  (secondary pool),  $Q_A Q_B^{2-}$  and  $Q_A^- Q_B H_2$  (lasts for 2–30 ms). The level P (300 ms) coincides with the maximum concentration of  $Q_A^- Q_B^{2-}$ , with the plastoquinone pool reduced. This level also reflects a balance between incident light at the PS II side and the utilization rate of the chemical (potential) energy and the rate of heat dissipation (Zhu et al., 2005). Rapid Light Curves (RLC) were performed using the pre-programmed LC1 protocol, which performs successive measurements of the sample  $\phi$ PS II under various light intensities (20, 50, 100, 200, 300, and 500  $\mu\text{mol photons m}^{-2} \text{s}^{-1}$ ) of continuous illumination, relating the rate of photosynthesis to PAR. From this analysis, several photochemical parameters were obtained (Table 1).

## Pigment Analysis

Pigments were extracted from cell sample pellets with 100% acetone and maintained in a cold ultra-sound bath for 2 min to

ensure complete disaggregation of the cell material. Temperature and time of extraction were  $-20^\circ\text{C}$  and 24 h in the dark, to prevent degradation (Cabrita et al., 2016, 2018; Feijão et al., 2018). Samples were then centrifuged for 15 min at  $4,000 \times g$  at  $4^\circ\text{C}$ . Dual beam spectrophotometer was used to scan supernatants from 350 nm to 750 nm, at 0.5 nm steps. The absorbance spectrum was introduced in the Gauss-Peak Spectra fitting library, using SigmaPlot Software. Pigment analysis was employed using the algorithm developed by Küpper et al. (2007). Thereby, Chlorophyll *a*, its trace element substituted forms, and Pheophytin *a* were detected.

## Fatty Acid Profiles and Lipid Peroxidation Products

Fatty acid analysis was performed by *trans*-esterification of cell pellets in freshly prepared methanol-sulfuric acid (97.5%, v/v) at  $70^\circ\text{C}$  for 60 min, as previously described in Feijão et al. (2018). Pentadecanoic acid (C15:0) was used as an internal standard. Fatty acids methyl esters (FAMES) were recovered using petroleum ether, dried under an  $\text{N}_2$  flow and re-suspended in an appropriate amount of hexane. One microliter of the FAME solution, obtained from each sample, was analyzed in a gas chromatograph (Varian 430-GC gas chromatograph) equipped with a hydrogen flame ionization detector set at  $300^\circ\text{C}$ . The temperature of the injector was set to  $270^\circ\text{C}$ , with a split ratio of 50. The fused-silica capillary column (50 m  $\times$  0.25 mm; WCOT Fused Silica, CP-Sil 88 for FAME; Varian) was maintained at a constant nitrogen flow of  $2.0 \text{ mL min}^{-1}$ , and the oven temperature was set at  $190^\circ\text{C}$ . FAs were identified by comparison of retention times with standards (Sigma-Aldrich), and chromatograms analyzed by the peak surface method using the Galaxy software (from whom?). The double bond index (DBI) and the omega 6/omega 3 ratios were calculated as follows:

$$DBI = \frac{2 \times (\% \text{ monoenes} + 2 \times \% \text{ dienes} + 3 \times \% \text{ trienes} + 4 \times \% \text{ tetraenes} + 5 \times \% \text{ pentaenes})}{100}$$

antification of lipid peroxidation products was performed by homogenizing cell samples in 10 % (v/v) trichloroacetic acid and brief sonication. Absorbance was recorded at 532 nm and 600 nm wavelengths, and the concentration of thiobarbituric acid reactive substances (TBARS) calculated using the molar extinction coefficient of  $155 \text{ mM}^{-1} \text{ cm}^{-1}$  (Heath and Packer, 1968).

## Antioxidant Enzymes Assay

All enzymatic assays were performed at  $4^\circ\text{C}$ . Pellets were suspended in 50 mM sodium phosphate buffer (pH 7.6) for extraction. Homogenates were centrifuged at  $10,000 \times g$  for 20 min (at  $4^\circ\text{C}$ ), and the supernatant was used for the enzymatic tests. Catalase (CAT) activity was measured by monitoring the consumption of  $\text{H}_2\text{O}_2$  and following the decrease in absorbance at 240 nm ( $\epsilon = 39.4 \text{ mM}^{-1} \text{ cm}^{-1}$ ) for two minutes, according to Teranishi et al. (1974). The reaction mixture (1 ml) contained 50 mM of sodium phosphate buffer (pH 7.6) and was started with the addition of 10  $\mu\text{l}$  of  $\text{H}_2\text{O}_2$  (15% v/v). Ascorbate peroxidase (APX) activity was determined by monitoring the decrease in

**TABLE 1** | Summary of fluorometric analysis parameters and their description.

OJIP-test	
AOECs	Active oxygen-evolving complexes
Area	Corresponds to the oxidized quinone pool size available for reduction and is a function of the area above the Kautsky plot
N	Reaction center turnover rate
$S_M$	Corresponds to the energy needed to close all reaction centers
$P_G$	Grouping probability between the two PSII units
ABS/CS	Absorbed energy flux per cross-section
TR/CS	Trapped energy flux per cross-section
ET/CS	Electron transport energy flux per cross-section
DI/CS	Dissipated energy flux per cross-section
RC/CS	Number of available reaction centers per cross-section
$TR_0/DI_0$	Contribution or partial performance due to the light reactions for primary photochemistry
$\delta_{RO}/(1-\delta_{RO})$	Contribution of PSI, reducing its end acceptors
$\psi_{EO}/(1-\psi_{EO})$	Equilibrium constant for the redox reactions between PS II and PS I
$RE_0/RC$	Electron transport from $PQH_2$ to the reduction of PS I end electron acceptors
RC/ABS	Reaction center II density within the antenna chlorophyll bed of PS II

absorbance at 290 nm and calculating the oxidized ascorbate, over two minutes of reaction time ( $\epsilon = 2.8 \text{ mM}^{-1} \text{ cm}^{-1}$ ; Tiryakioglu et al., 2006). The reaction mixture contained 50 mM of sodium phosphate buffer (pH 7.0), 2 mM of  $\text{H}_2\text{O}_2$ , 0.1 M L-ascorbate, and 100  $\mu\text{L}$  of pellet extract. The reaction was initiated by addition of ascorbate. Glutathione reductase (GR) activity was tested by measuring for 180 s the decrease in absorbance (at 340 nm) caused by glutathione-dependent NADPH oxidation (Foyer and Halliwell, 1976). The reaction mixture (1 ml) contained 50 mM phosphate buffer (pH 7.6), 1 mM EDTA, 5 mM glutathione oxidized (GSSG), 1.2 mM NADPH and cell extract. The reaction started by adding NADPH and the activity was calculated by using an extinction coefficient of  $6.2 \text{ mM}^{-1} \text{ cm}^{-1}$ . Superoxide dismutase (SOD) activity was tested by monitoring the reduction of pyrogallol at 325 nm (Marklund and Marklund, 1974). The reaction mixture (1 ml) contained 50 mM of sodium phosphate buffer (pH 7.0), 3 mM of pyrogallol, in order to start the reaction, Milli-Q water (18.2 M $\Omega$  cm), and 10  $\mu\text{l}$  extract. To evaluate substrate auto-oxidation, controls were assayed without substrate, as described elsewhere.

## Statistical Analysis

Following normality and homogeneity tests of data, analysis of variance (factorial ANOVA) was applied using the Stat-Soft Inc. STATISTICA version 10 software was used to test for significant differences in effects among control and Cu- and CuO ENP-exposed *P. tricornutum* cells. Fisher's *post-hoc* test was performed in order to investigate significant differences among means. Spearman rank correlation was used to highlight the strength and direction of the relationship between parameters. Significance was set at  $p < 0.05$ .

## RESULTS

### Cell Growth

Exposure of *P. tricornutum* cells to low ( $1 \mu\text{g L}^{-1}$ ), medium ( $5 \mu\text{g L}^{-1}$ ), and high ( $10 \mu\text{g L}^{-1}$ ) concentrations of Ionic Cu and CuO ENPs during the treatment period resulted in an overall decrease of both biomass (expressed as cell density) and specific growth rate. Cells exposed to CuO ENPs displayed a steeper decrease in cell density with increasing metal concentrations when compared to free Cu-exposed cells (Figures 1A,B). This decrease is evaluated throughout the cell growth curves derived parameters. Differences in specific growth rates between Cu-ionic and CuO ENP exposed cells treatments were only significant ( $p < 0.05$ ) at maximum tested concentration levels ( $10 \mu\text{g L}^{-1}$ ; Figure 1E). The number of divisions per day ( $M$ , Figure 1D) and doubling time ( $d$ , Figure 1C) reflected the decline found in the specific growth rate, and again, significant differences ( $p < 0.05$ ) between the control and the highest level of CuO ENPs ( $10 \mu\text{g L}^{-1}$ ). In sum, CuO ENPs inhibited diatom growth rate.

### Cell Metal Content and Nanoparticle Characterization and Metal Release

Elemental analysis revealed different trends in copper content between the tested groups Cu Ionic form and CuO ENPs

(Figure 2A). Cell Cu content was higher in cells exposed to Ionic Cu concentrations of 1 and  $5 \mu\text{g L}^{-1}$ , and lower following exposure to  $10 \mu\text{g L}^{-1}$ . Cu ENPs treatments showed increasing uptake of Cu in the cells with increasing concentrations, albeit more evident in cells exposed to  $10 \mu\text{g L}^{-1}$  of Cu nanoparticles ( $p < 0.05$ ). This suggested that CuO was less bioavailable, except for the higher concentration employed. Cell Cu content was positively correlated with nanoparticle concentration ( $r^2 = 0.80$ ,  $p < 0.05$ ), Cu-substituted chlorophyll *a* ( $r^2 = 0.85$ ,  $p < 0.05$ ), total content of FAs ( $r^2 = 0.79$ ,  $p < 0.05$ ) and with TBARs ( $r^2 = 0.87$ ,  $p < 0.05$ ). This Cu uptake will later be discussed in relation to its physiological implications.

Copper concentrations in the test units exposed to the nanoparticle form were also surveyed along an equivalent exposure period (Figure 2B). The Cu content of the collected water samples showed that there were no significant fluctuations of the Cu levels either between concentrations or along with the considered time trial.

The zeta potential of the Cu ENPs determined by DLSS was found to be  $-7.30 \pm 3.72 \text{ mV}$ . Cu ENP size distribution could not be determined with DLSS due to agglomeration of the particles; however, electron micrograph confirmed size distribution as indicated by the supplier (Supplementary Figures 1A–D). Particle elemental composition and X-ray fluorescence spectra was obtained from the Cu ENPs in *f/2* medium using by TXRF as abovementioned (S2 PICOFOX, Bruker, Germany; Supplementary Figure 1E). X-ray fluorescence spectrum analysis revealed high amounts of Cu in Cu ENPs suspension as well as of other minor elements, derived from the *f/2* medium composition.

### Primary Photochemistry

The photochemical processes underlying carbon and light-harvesting and thus biomass production were investigated with non-invasive PAM chlorophyll fluometry. RLC measurements in dark-adapted cells exposed to ionic copper and CuO ENPs evidenced increased relative electron transport rates (rETR) along the thylakoid membrane, observable at  $200 \mu\text{mol photons m}^{-2} \text{ s}^{-2}$  (Figures 3A,B). These results were consistent with the increased photosynthetic efficiency ( $\alpha$ , Figure 3C) and the maximum electron transport rate ( $\text{ETR}_{\text{max}}$ ) of Cu exposed cells when compared to control cells (Figure 3D). Regarding respiratory efficiency ( $\beta$ , Figure 3E), an increase at low concentrations ( $1 \mu\text{g L}^{-1}$ ) and a successive decrease at higher concentrations ( $5$  and  $10 \mu\text{g L}^{-1}$ ) were observed for both cells exposed to ionic and ENP Cu forms. Photosynthetic efficiency was also found to correlate with increased percentage of tri-unsaturated hexadecatrienoic acid (C16:3;  $r^2 = 0.70$ ,  $p < 0.05$ ) in *P. tricornutum* cells exposed to CuO ENPs. Analysis of strong actinic light induced OJIP fluorescence transients (JIP-test) showed considerable differences in dark-adapted cells. Differences were found in cells exposed to CuO ENPs affecting the shape of the Kautsky curve (Figures 4A,B), which gives a general view on the structure, conformation, and function of photosynthetic apparatus, especially focusing on the PS II. Considering these aspects of the photosynthetic process, a further investigation was conducted focusing on the compartments of the photochemical apparatus.

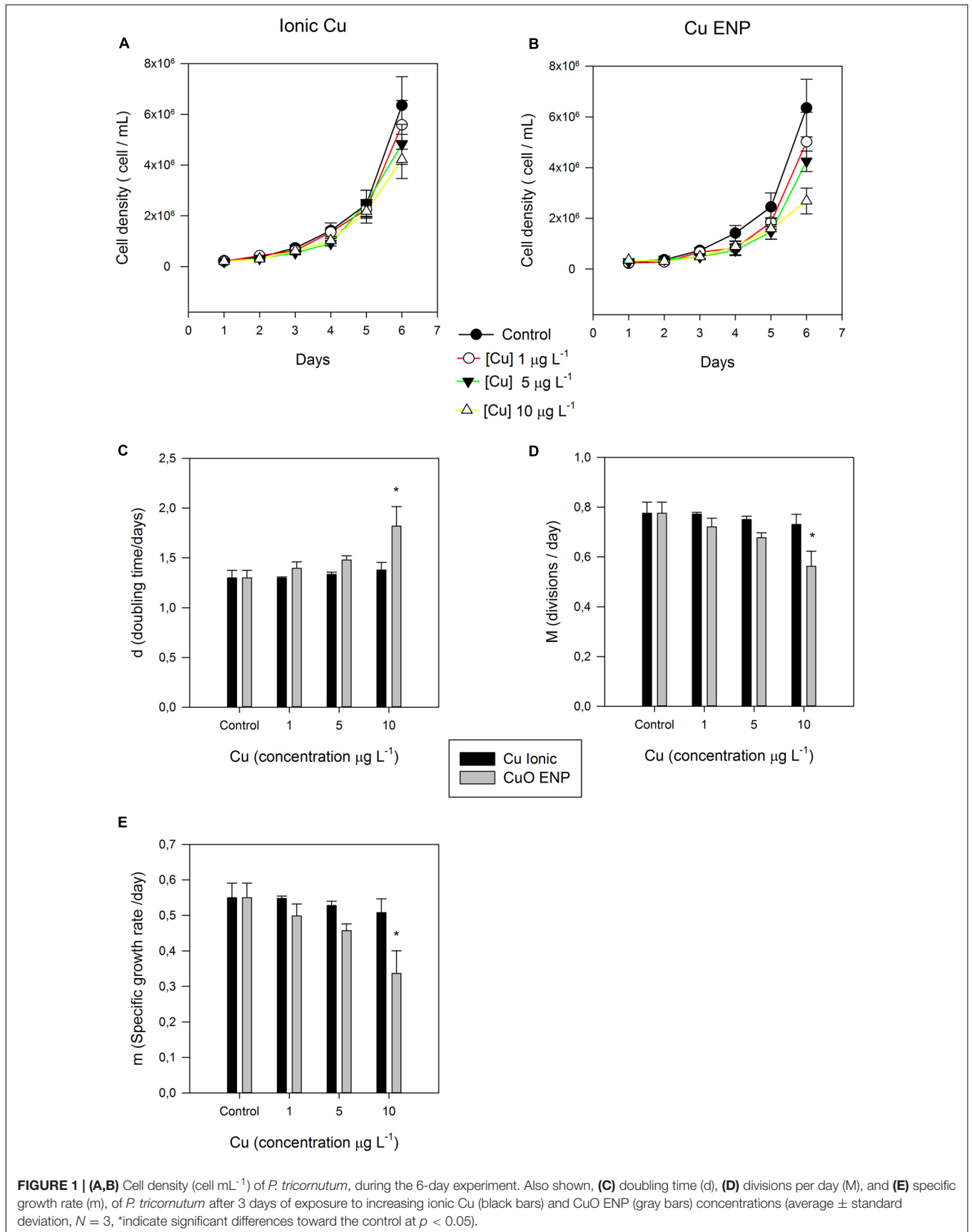
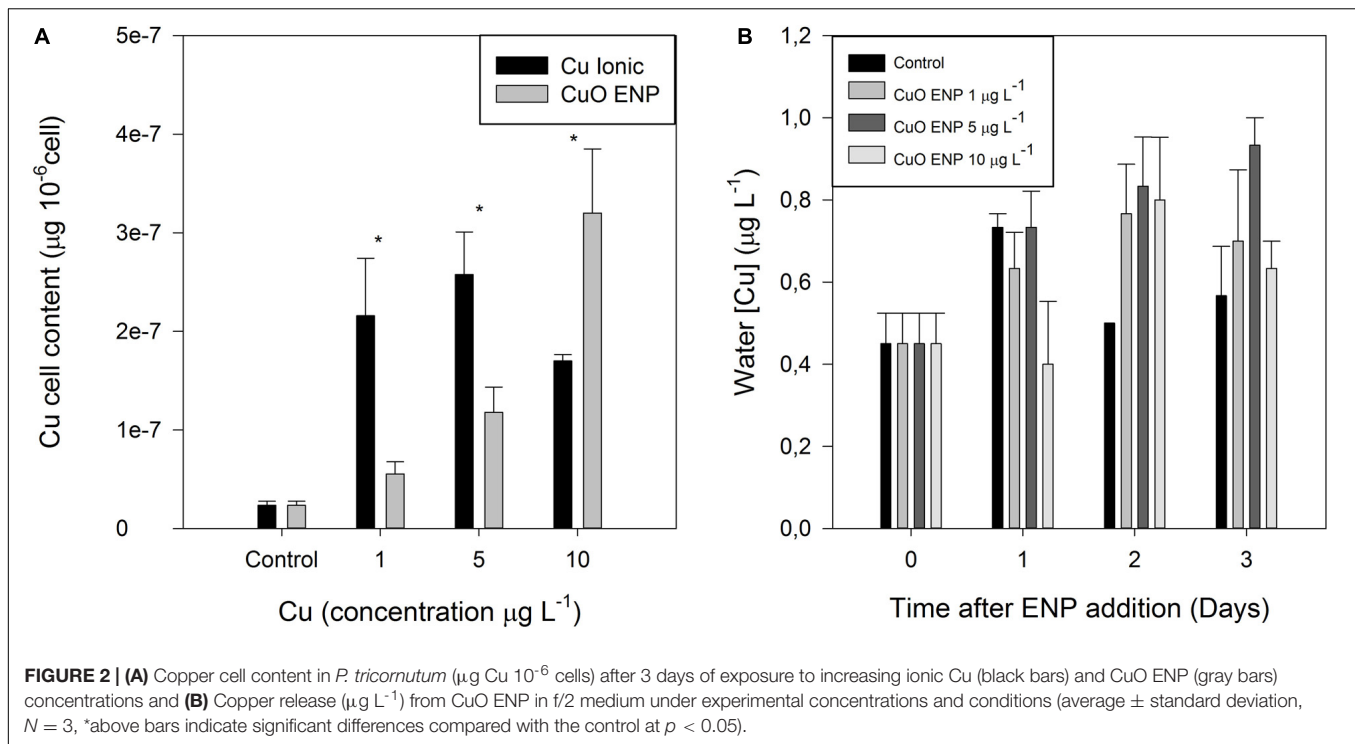


**FIGURE 1 | (A,B)** Cell density (cell mL<sup>-1</sup>) of *P. tricornutum*, during the 6-day experiment. Also shown, **(C)** doubling time (d), **(D)** divisions per day (M), and **(E)** specific growth rate (m), of *P. tricornutum* after 3 days of exposure to increasing ionic Cu (black bars) and CuO ENP (gray bars) concentrations (average ± standard deviation, N = 3, \*indicate significant differences toward the control at p < 0.05).



The size of the oxidized quinone pool (**Figure 4C**) was significantly higher ( $p < 0.05$ ) in cells under low ( $1 \mu\text{g L}^{-1}$ ), medium ( $5 \mu\text{g L}^{-1}$ ), and high concentration ( $10 \mu\text{g L}^{-1}$ ) of CuO ENPs, compared to control treatments. The same was observed at medium and high concentrations of ionic Cu. Regarding the energy necessary to close all RCs (**Figure 4D**), cells exposed to all concentration levels of CuO ENPs showed a significant increase ( $p < 0.05$ ) compared to control cells, as well as for cells treated with medium and high concentrations of ionic Cu. A similar trend was observed for the total number of electrons transferred in the electron transport chain (**Figure 4E**), which significantly increased in cells exposed to medium and high concentrations of ionic Cu, and more markedly to all concentrations of CuO ENPs when compared to control cells. Connectivity between PS II antennae ( $P_G$ , **Figure 4F**) was found to be significantly lower ( $p < 0.05$ ) in cells exposed to all levels of both Cu forms. Moreover, a positive correlation was found between  $P_G$  and the reduction in the long-chain (LC) PUFA EPA (C20:5) content ( $r^2 = 0.79$ ,  $p < 0.05$ ) in the cells subjected to CuO ENPs.

Analyzing OJIP-derived energy transduction fluxes on a cross-section basis in dark-adapted samples (**Figures 5A,B**), differences between ionic Cu and CuO ENPs, and between concentrations were identified. The absorbed (ABS/CS), trapped (TR/CS), transported (ET/CS) energy fluxes and the number of available reaction centers per cross-section (RC/CS) were significantly lower ( $p < 0.05$ ) in cells exposed to increasing concentrations of CuO ENP treatment ( $p < 0.05$ ; **Figure 5B**), compared to either control or ionic- Cu exposed cells. ABS/CS was also found negatively correlated with the content of C16:3 ( $r^2 = -0.81$ ,  $p < 0.05$ ). Regarding the dissipated energy fluxes (DI/CS), only CuO ENP exposure led to an increase in this parameter

as a function of concentration, while ionic- Cu exposed cells showed only slight changes with increasing concentrations. All these changes in the several processes and compartments of the photochemical apparatus and in the energy transduction pathway propose possible changes at the biochemical level.

## Pigment Profiles

Considering photochemical changes mentioned before, the composition of light-harvesting pigments was evaluated. Changes in the content of Chlorophyll *a* (MgChl *a*), Pheophytin *a* (Pheo *a*) and Cu-substituted chlorophyll *a* (CuChl *a*) were observed in cells of *P. tricornutum* exposed to CuO ENPs (**Figure 6**). A reduction in total MgChl *a* level with increasing concentrations of CuO ENPs was detected, along with a significant rise ( $p < 0.05$ ) in the Pheo *a* and CuChl *a* content in cells exposed to  $10 \mu\text{g L}^{-1}$  CuO ENPs ( $p < 0.05$ ), suggesting a role of Cu nanoparticles in promoting the  $\text{Mg}^{2+}$  substitution in the main photosynthetic pigments. In fact, increased Cu-substituted Chl *a* contents correlated with CuO ENP concentrations ( $r^2 = 0.73$ ,  $p < 0.05$ ). In the ionic Cu exposed cells, changes in MgChl *a*, Pheophytin *a* and CuChl *a* content triggered by increasing Cu levels were not significant (**Figure 6**).

## Fatty Acid Profiles

Fatty acid profiles were also conducted. Analysis of the composition and contents of FAs in *P. tricornutum* cells showed significant changes between control and copper exposed cultures (**Figure 7A**). The most relevant differences were found in EPA (20:5) and hexadecatrienoic acid (16:3) relative amounts, for cells subject to CuO ENPs in all tested concentrations. A significant decrease ( $p < 0.05$ ) in EPA (20:5) relative abundance

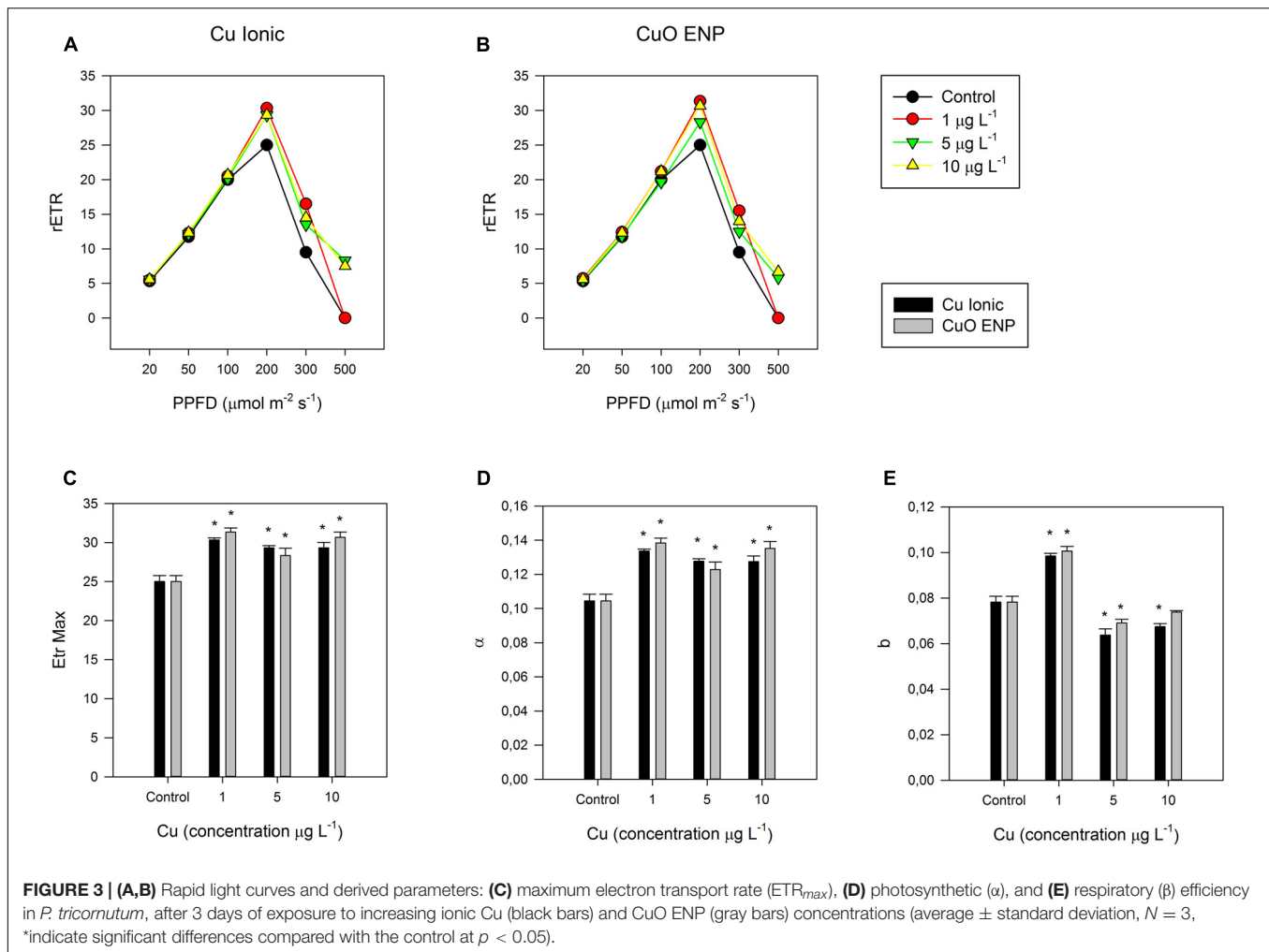


**FIGURE 3 | (A,B)** Rapid light curves and derived parameters: **(C)** maximum electron transport rate ( $\text{ETR}_{\text{max}}$ ), **(D)** photosynthetic ( $\alpha$ ), and **(E)** respiratory ( $\beta$ ) efficiency in *P. tricornutum*, after 3 days of exposure to increasing ionic Cu (black bars) and CuO ENP (gray bars) concentrations (average  $\pm$  standard deviation,  $N = 3$ , \*indicate significant differences compared with the control at  $p < 0.05$ ).

was observed combined with a significant rise ( $p < 0.05$ ) in hexadecatrienoic acid (16:3). Palmitic acid (16:0) and the monounsaturated palmitoleic acid (16:1) ratios in cells exposed to medium and high concentrations of ionic Cu and CuO ENPs. Moreover, stearidonic acid (18:4  $n-3$ ) was reduced for ionic Cu and CuO ENPs at all concentrations, whereas C16:4 content only increased ( $p < 0.05$ ) in cells exposed to CuO ENPs. Exposure to CuO ENPs also caused a decline in the gamma-linolenic acid (18:3  $n-6$ ) content of the cells. The higher content of C16:3 and C16:4 was correlated with the energy necessary to close all reaction centers ( $\text{Sm}$ ;  $r^2 = 0.80$  and  $0.81$ , respectively,  $p < 0.05$ ) and with the total number of electrons transferred in the ETC ( $r^2 = 0.81$  in both cases,  $p < 0.05$ ). Modifications in the FA composition resulted in a significant increase ( $p < 0.05$ ) in the DBI (**Figure 7B**), albeit only at the highest concentration of CuO ( $10 \mu\text{g L}^{-1}$ ), and in a higher omega 6/omega 3 ratio (**Figure 7D**) for all CuO ENP concentrations. Regarding total FAs content on a cell number basis, a significant increase ( $p < 0.05$ ) was observed in cells exposed to CuO ENPs at the highest concentration ( $10 \mu\text{g L}^{-1}$ ; **Figure 7C**).

Considering FA saturation classes, the percentage of saturated and monounsaturated FAs was significantly reduced ( $p < 0.05$ ),

while a significant rise ( $p < 0.05$ ) in the percentage of polyunsaturated and unsaturated FAs were observable for CuO ENP exposure (**Figure 8A**). Ratios of unsaturation/saturation and polyunsaturation/saturation reflected the abovementioned results on FA composition, with a significant increase of unsaturation and an overall reduction in saturation for CuO ENP exposure (**Figures 8A,B**). Cells exposed to CuO ENPs showed an overall higher stress effect on FA content in comparison with ionic Cu effects.

## Stress Biomarkers

Considering the overall changes in the energetic and biochemical level abovementioned, the cellular oxidative stress levels were tested with enzymatic antioxidant assays. Antioxidant enzymes assays evidenced an overall increase in enzyme activity under nano Cu experimental conditions (**Figures 9A–D**). Specifically, APX and GR, which showed an increase in activity values along the gradient of Cu concentration, with more pronounced responses in cells exposed to CuO ENPs. In contrast, CAT and SOD activity were less evident with increasing Cu concentration, and the highest enzyme activity was measured at medium Cu concentration ( $5 \mu\text{g L}^{-1}$ ). Compared to control cells, the

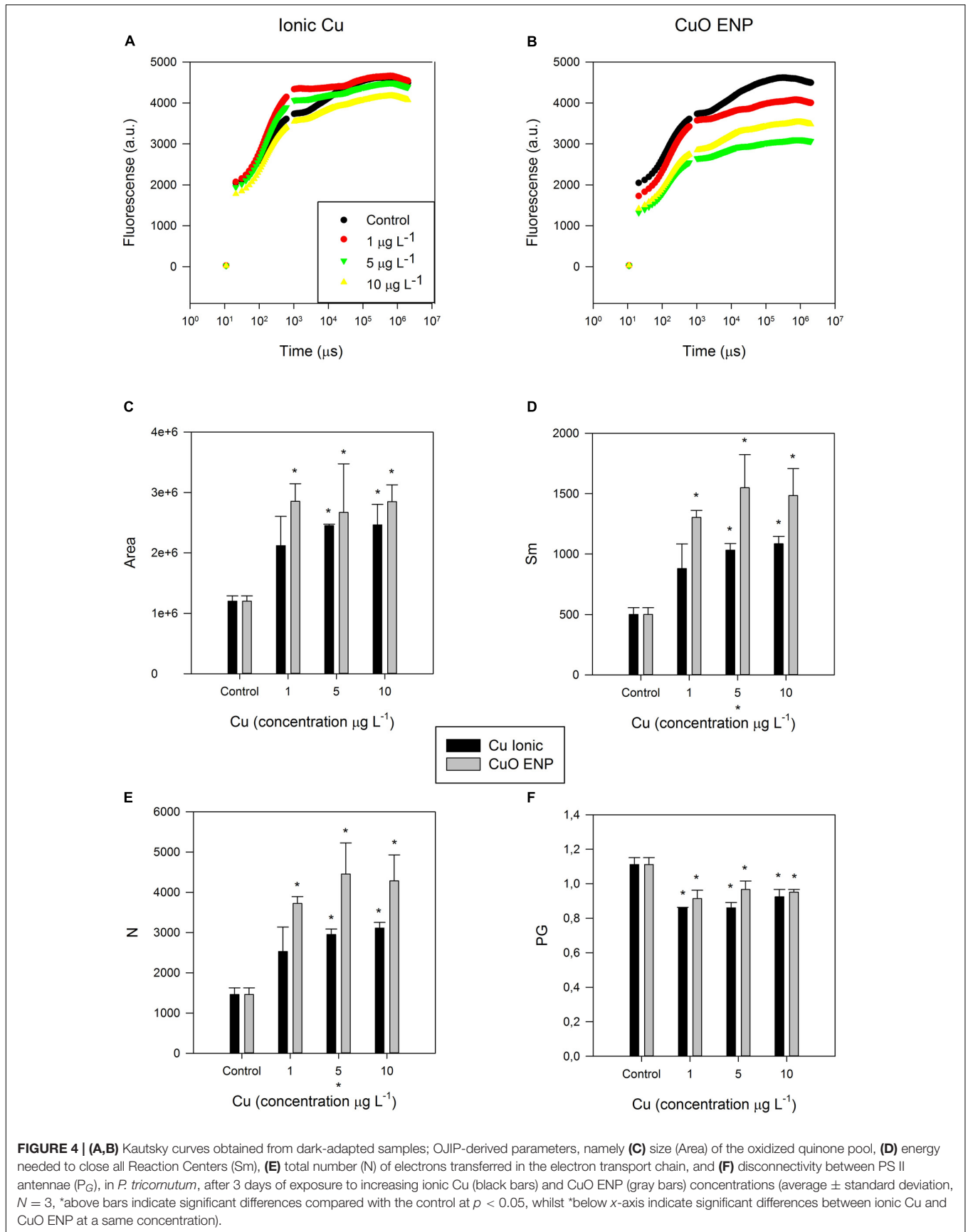
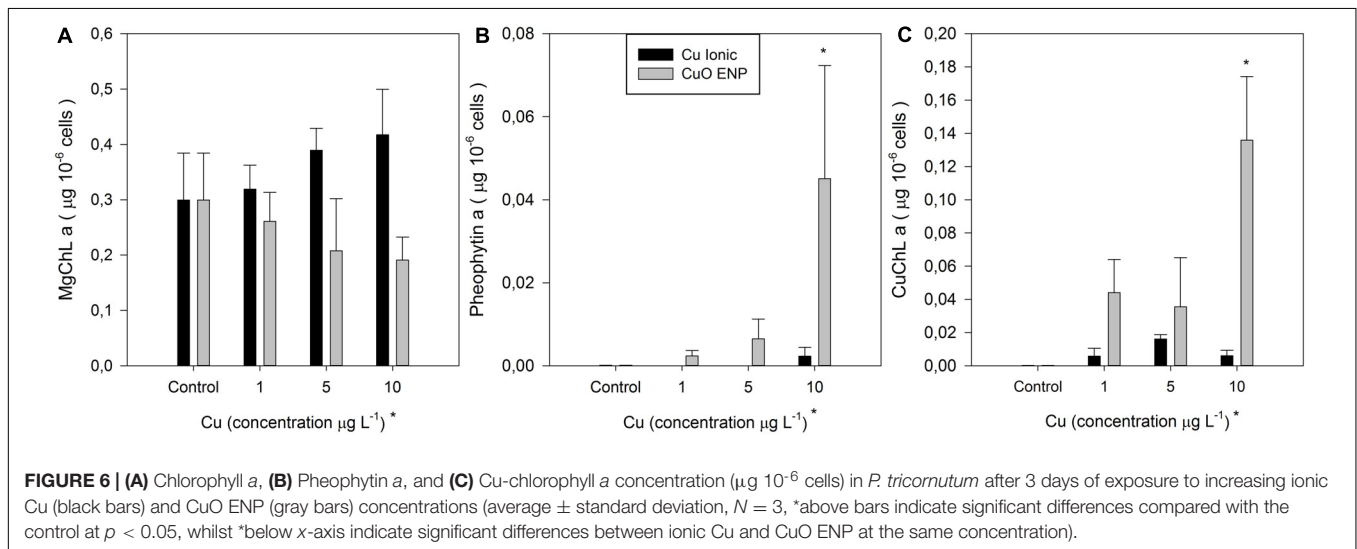
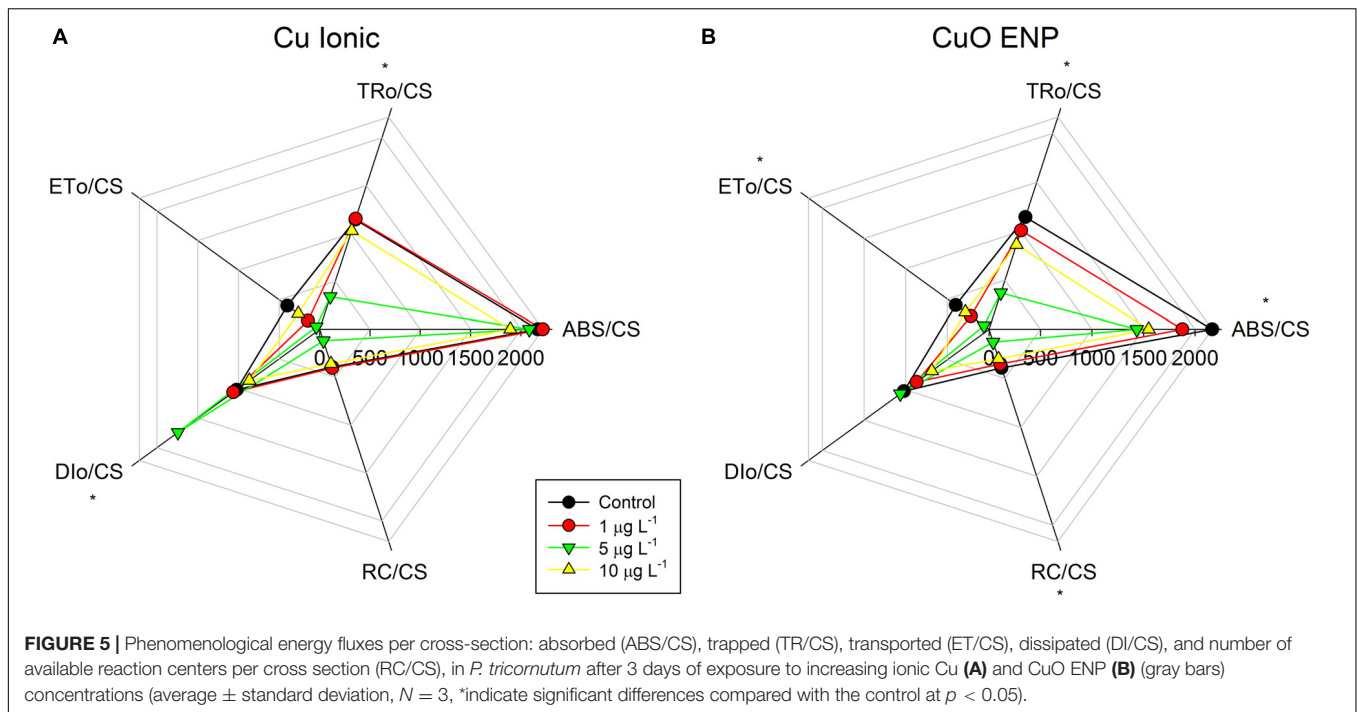


**FIGURE 4 | (A,B)** Kautsky curves obtained from dark-adapted samples; OJIP-derived parameters, namely **(C)** size (Area) of the oxidized quinone pool, **(D)** energy needed to close all Reaction Centers (Sm), **(E)** total number (N) of electrons transferred in the electron transport chain, and **(F)** disconnectivity between PS II antennae (PG), in *P. tricornutum*, after 3 days of exposure to increasing ionic Cu (black bars) and CuO ENP (gray bars) concentrations (average ± standard deviation, N = 3, \*above bars indicate significant differences compared with the control at p < 0.05, whilst \*below x-axis indicate significant differences between ionic Cu and CuO ENP at a same concentration).

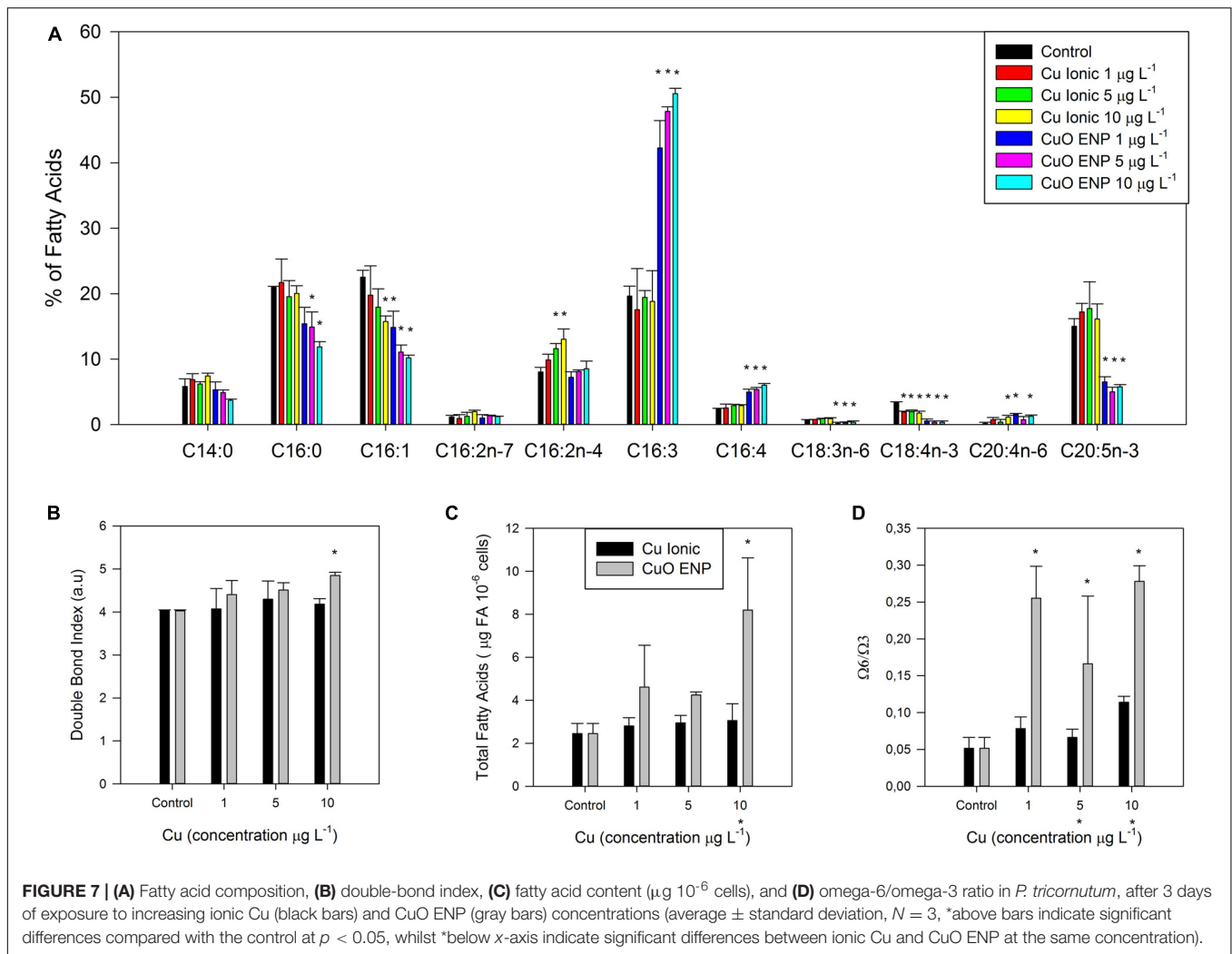


TBARs total content in exposed cells was significantly enhanced ( $p < 0.05$ ) at the highest CuO ENP concentration ( $10 \mu\text{g L}^{-1}$ ; Figure 9E).

## DISCUSSION

Overall results show that exposure to non-lethal concentrations of copper engineered nanoparticles (CuO ENPs) resulted in the reduced fitness of a marine model diatom, *P. tricornutum*, and elicited higher toxicity than its ionic form counterpart. Biomarkers, as specified below, appeared to be sensitive to MeENPs stress in this species. In general, changes in cell growth,

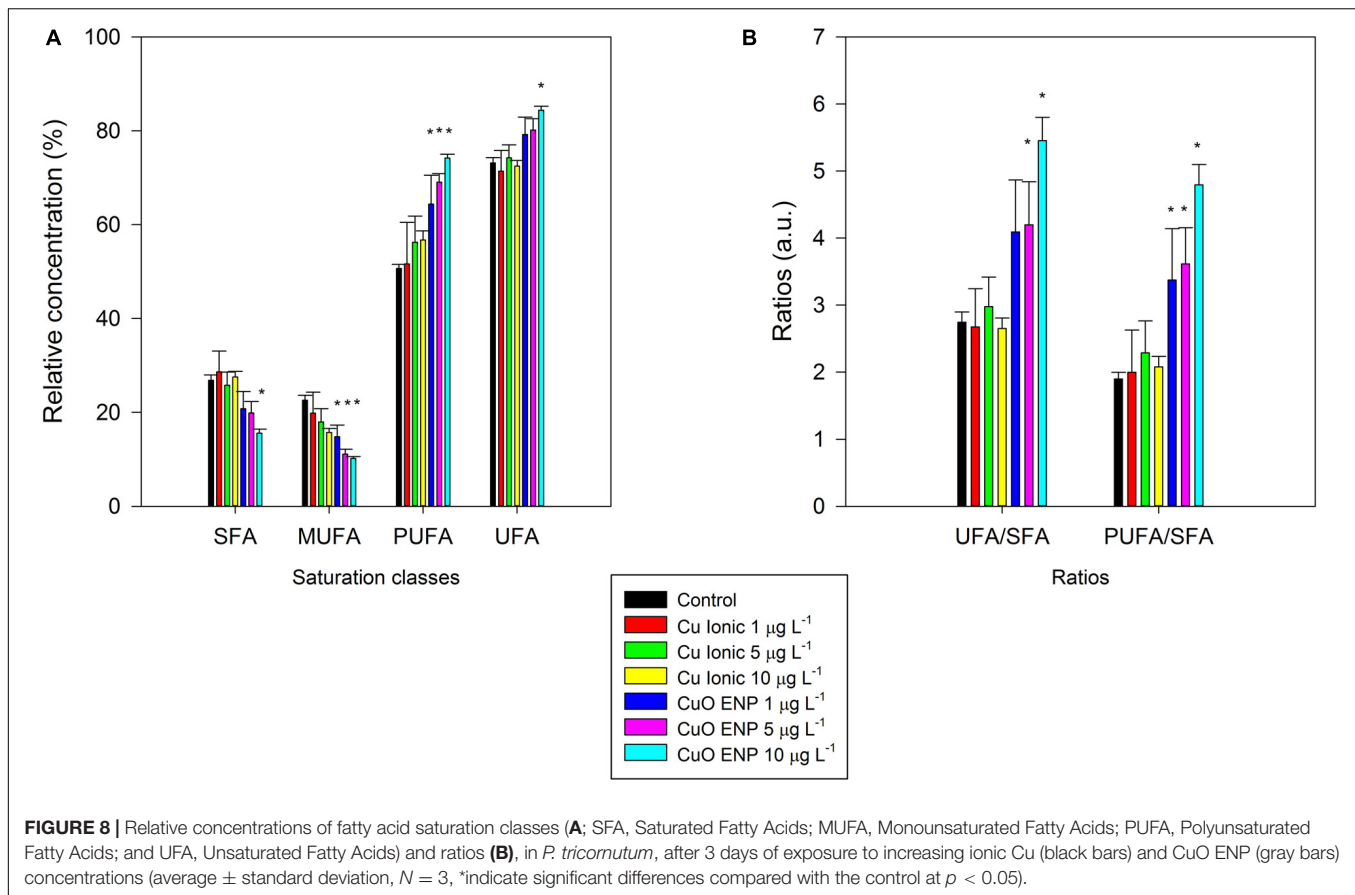
photosynthesis, pigment content, FA production, and oxidative stress metabolism, as well as the production of Cu-substituted chlorophylls, were observed for diatoms exposed to all tested Cu concentrations. However, effects were more pronounced for CuO ENPs exposure than for direct ionic Cu, in particular at the highest tested CuO ENP concentration. Although previous studies show that ionic copper can be released from CuO ENPs (Zhang et al., 2018), in our experimental conditions no significant fluctuations could be observed in the dissolved copper levels along with the exposure in reactors containing Cu ENPs. Thus all comparisons discussed here base on the initial form of copper introduced into the culture medium, assuming that there is no Cu transition from nanoparticle to ionic form as observed



in the water Cu concentrations results. Cell growth was not significantly reduced in cells exposed to ionic Cu in comparison to the control group, which is in line with previous results reported for *P. tricornutum* at similar metal concentrations (Cabrita et al., 2016, 2018). In contrast, cell growth decreased as a function of exposure to CuO ENP, with significant inhibition at high concentrations ( $10 \mu\text{g L}^{-1}$ , corresponding to  $0.13 \mu\text{M}$ ; add  $p$  values here). This is in agreement with previous studies that showed that CuO ENPs in antifouling paints could cause severe growth inhibition in different algal species, including *P. tricornutum* (Anyago et al., 2008; Zhang et al., 2018). Additionally, Zhang et al. (2018) also observed severe growth inhibition in *Skeletonema costatum* under the exposure to Cu ENPs, pointing out the release of ionic Cu from the ENPs as the principal cause for the verified growth inhibition. On the other hand, Zhu et al. (2017) only found inhibition of *P. tricornutum* growth at both ionic Cu and Cu ENP concentrations of  $20 \mu\text{M}$  and above. The observed impact of CuO ENPs compared to that of ionic Cu on *P. tricornutum* growth can be explained by the fact that CuO ENPs cause cytotoxicity via the release of  $\text{Cu}^{2+}$  into the culture medium (Horie et al., 2012). This ion release is

increased for particles  $< 50 \text{ nm}$  (Anyago et al., 2008), which was the size of the CuO ENPs used in this study (here link the SEM image). Furthermore, CuO ENPs can be about 140-fold more bioavailable than its ionic form (Aruoja et al., 2009), which supports the higher inhibitory effect on *P. tricornutum* growth from CuO ENPs compared to the ionic form.

Excess copper is an important inhibitor of photosynthesis (Cid et al., 1995). Copper affects the PS II activity at the Pheo- $\text{Q}_\text{A}^-$  domain (Küpper et al., 2002), inhibiting the electron transport through damage to the donor and the acceptor sides of PS II (Patsikka et al., 1998). Accordingly, Cid et al. (1995) suggested that  $\text{Cu}^{2+}$  can be responsible for the inactivation of PS II reactions centers. Mohanty et al. (1989) proposed that  $\text{Cu}^{2+}$  inhibits PS II photochemistry, primarily affecting the functionality of the secondary quinone electron acceptor,  $\text{Q}_\text{B}$ , not only by blocking the electron transport but also by modifying and inactivating the  $\text{Q}_\text{B}$  site. Exposure to either ionic Cu or CuO ENPs leads to an increase in maximum  $\text{ETR}_{\text{max}}$  and photosynthetic efficiency ( $\alpha$ ), corresponding to a higher amount of oxidized quinones, as well as to a decrease in electron transport energy flux per cross-section ( $\text{ET}_0/\text{CS}$ ), which suggests



a malfunction between elements of PS II (Duarte et al., 2016). The positive correlation between photosynthetic efficiency and the higher percentage of tri-unsaturated hexadecatrienoic acid (C16:3) in *P. tricornutum* cells exposed to CuO ENP, as observed in this study, suggests a potential mechanism to counteract stress in photosynthesis, as this FA is only found in plastidial lipids, mainly in monogalactosyldiacylglycerol (MGDG), which forms the bulk of thylakoid lipids (Feijão et al., 2018). The larger size of the oxidized quinone pool, and the higher level of energy, needed to close the reaction centers, as evidenced by cells exposed to CuO ENPs, indicate that efficient energy transport is required (Feijão et al., 2018), which if reduced, suggests probable damage in the quinone pool electron transport (Duarte et al., 2017; Cabrita et al., 2018). However, no evidence of enhanced dissipation energy flux was observed. The above-mentioned changes in photosynthetic parameters could thus be due to changes in the grouping probability ( $P_G$ ), which is a direct measure of the connectivity between the PS II antennae. The decrease found for this index in the presence of both ionic Cu and CuO ENPs, indicates a decreased connectivity between the two PS II units and a probable impairment of energetic transport (Duarte et al., 2016). EPA is highly abundant in glycolipids and phospholipids that form the chloroplast membranes lipids, like MGDG and phosphatidylglycerol (PG), and changes in the FAs composition in chloroplast membrane lipids can explain photosynthesis imbalances, through modifications of the redox

potential (Kern and Guskov, 2011). Previous studies reported that changes in the FA composition of polar lipids can be one of the causes of dimerization of PS II (Kruse et al., 2000), as suggested also from the correlation between disconnectivity in PS II antennae and the reduction in EPA content found in cells exposed to CuO ENPs. The higher number of electrons transferred in the electron transport chain (turnover number,  $N$ ) was not reflected in an effective trapping energy flux (TR/CS) in cells exposed to CuO ENPs. Instead, the detected reduction in the density of reaction centers (RC/CS) corresponded to a higher number of inactive reaction centers, and to a lowered ability to reduce the primary electron acceptor  $Q_A$ . This could be confirmed by the low absorbed photon flux (ABS/CS) and the higher size in the oxidized quinone pool found in CuO ENP exposed *P. tricornutum* cells. Nevertheless, no changes were detected in the net rate of closure of PS II RC ( $M_o$ ) and in the energy needed to close all RCs, which were expected to counteract the inactive RCs (Duarte et al., 2016). Even though trapped energy flux diminished in the ionic Cu exposed cells, little changes were detected in energy dissipation. Overall, changes in photobiology were more evident for *P. tricornutum* subjected to CuO ENPs, suggesting a negative impact of CuO ENPs on PS II functionality or integrity of light harvesting complexes.

This was further promoted by the observation that the content of the light-harvesting pigments and its substituted form also

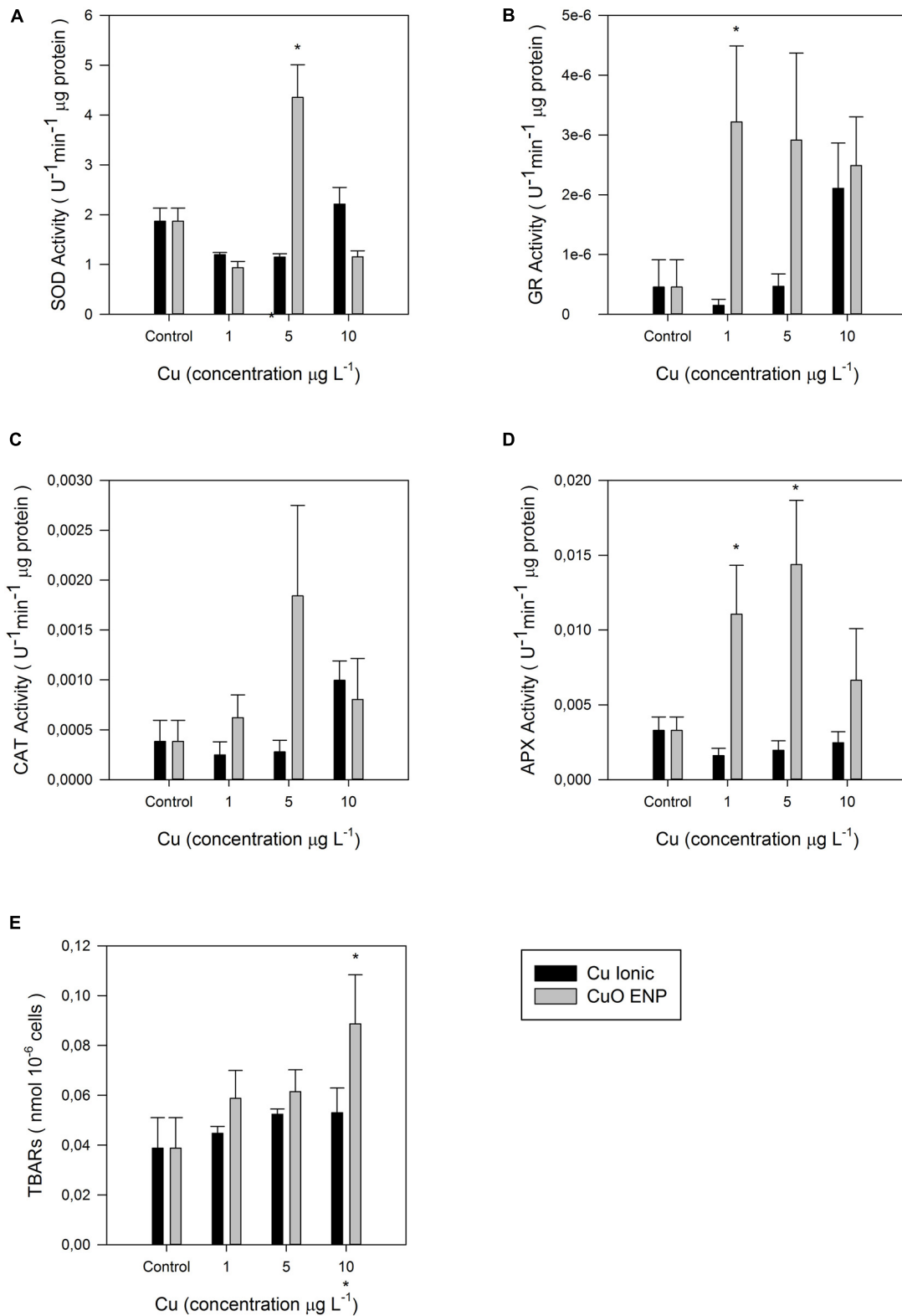


**FIGURE 9 |** Enzymatic activities: **(A)** Superoxide dismutase (SOD), **(B)** glutathione reductase (GR), **(C)** catalase (CAT), **(D)** ascorbate peroxidase (APX) in  $U^{-1} \mu g$  protein, and **(E)** lipid peroxidation measured as concentration of thiobarbituric acid reacting substances (TBARs; nmol  $10^{-6}$  cells), in *P. tricornutum* after 3 days of exposure to increasing ionic Cu (black bars) and CuO ENP (gray bars) concentrations (average  $\pm$  standard deviation,  $N = 3$ , \*above bars indicate significant differences compared with the control at  $p < 0.05$ , whilst \*below x-axis indicate significant differences between ionic Cu and CuO ENP at the same concentration).

changed, mostly for *P. tricornutum* exposed to CuO ENPs at the highest concentration ( $10 \mu\text{g L}^{-1}$ ). The decrease in MgChl *a* along the CuO ENP concentration gradient can be partially explained by direct replacement with CuChl *a*, which was highly significant for *P. tricornutum* exposed to the highest tested level of CuO ENPs. In parallel, a significant enhanced amount of Pheophytin *a*, the main product of degradation of MgChl *a* was observed. This is in agreement with previous findings reported by Zhang et al. (2018), where a similar depletion in Chl-*a* was also detected and attributed to destruction of this molecule promoted by Cu. The formation of CuChl *a* in cells exposed to both ionic Cu and CuO ENPs corroborates previous findings showing the occurrence of this substituted chlorophylls in *P. tricornutum* exposed to ionic Cu (Cabrita et al., 2018). It is already known that the central  $\text{Mg}^{2+}$  ion of chlorophyll can be substituted by trace metals, such as Cu, and constitutes an important part of the damage occurring in metal-stressed photosynthetic organisms (Küpper and Spiller, 1998; Küpper et al., 2002). As a matter of fact, Cu-substituted Chl *a* was found positively correlated with CuO ENP concentration in this study. Excess levels of this substituted and far less efficient chlorophyll form (CuChl *a*) can partly explain the decrease in efficiency in the absorbing photon flux, and in the ability for trapping and transporting energy, reducing PS II overall capacity.

The FA profiles of lipids from *P. tricornutum*, which are characterized by a high diversity of FAs and distinct signatures for different lipid classes (Abida et al., 2015; Yang et al., 2017; Feijão et al., 2018), was strikingly changed by CuO ENPs, even at the lowest concentration tested ( $1 \mu\text{g L}^{-1}$ ). Ionic copper had no particular impact on FA profiles neither on total content, most probably because the employed concentrations used were not sufficiently high to cause stress. Given that, the most remarkable changes induced by CuO ENPs involved the LC-PUFAs contained in glyco- and phospholipids, typical of chloroplast membranes of this diatom like mono- and digalactosyldiacylglycerol (MGDG, DGDG), phosphatidylcholine (PC) and PG. EPA is usually found in high levels in *P. tricornutum* (Dunstan et al., 1993; Feijão et al., 2018), and is part of all membrane lipids but almost absent in triacylglycerol (TAG; Arao et al., 1987), and its significant decrease with exposure suggests probable membrane damage. A reduction in EPA content associated with the membrane lipids has also been found in *P. tricornutum* under other types of stress, such as heat (Feijão et al., 2018) and nitrogen starvation (Remmers et al., 2017). The notable decline in EPA content occurred in parallel with a significant rise in both the percentage of tri-unsaturated hexadecatrienoic acid (C16:3) and tetra-unsaturated hexadecatetraenoic acid (C16:4). These FAs are synthesized by successive desaturations of monounsaturated palmitoleic acid (C16:1) in the inner membrane of the chloroplast (Dolch and Maréchal, 2015), and almost exclusively contained in MGDG (Abida et al., 2015; Popko et al., 2016). The enhancement in C16:3 and C16:4, found positively correlated with the energy necessary to close all reaction centers and with the total number of electrons transferred in the ETC can be a possible way for *P. tricornutum* to counteract changes in photosynthesis associated with Cu stress, by increasing the efficiency in transport

along the electron transport chain. Nevertheless, the absorption energy flux was negatively correlated with the content of C16:3; maybe to maintain an efficient energy flow. Alterations in FA composition and the influence of unsaturation on membrane properties connected to photosynthetic performance has already been highlighted in studies over cation-imposed stress in photosynthetic organisms (Allakhverdiev et al., 1999, 2001; Duarte et al., 2017; Cabrita et al., 2018).

The decrease in the content of palmitic acid (C16:0) and palmitoleic acid (C16:1) is likely related to its intensive desaturation to produce C16:3 and C16:4 (Dolch and Maréchal, 2015) to support thylakoid membrane functioning so that cells could cope with CuO ENP stress. However, a decrease in these saturated and mono-unsaturated FA is often associated with a reduction in the content of storage lipids. Although they are present in all lipid classes, C16:0 and C16:1 are quite abundant in diatom triacylglycerols, accounting for nearly 100% of the total FAs at the *sn*-2 position of these storage lipids (Li et al., 2014). This possible decrease in TAG amounts would not be in accordance with other studies, in which storage lipids accumulate under stress conditions (Sharma et al., 2012). However, TAG accumulation in this study cannot be excluded since, under stress conditions such as nitrogen deprivation, FA composition can be altered by the incorporation of FA from membrane lipids (Remmers et al., 2017). Indeed, Shen et al. (2016) found that the content of C16:1 decreases dramatically in phospholipids and remains largely unchanged in glycolipids in *P. tricornutum* under nitrogen starvation, suggesting that C16:1 is not specific to TAGs and cannot serve as a characteristic FA of TAGs. Further investigation on TAG and membrane lipid classes content and FAs compositions in *P. tricornutum* cells exposed to CuO ENPs is necessary to elucidate this question. Further research to understand the mechanisms behind changes in lipids triggered by CuO ENPs in association with their location and function in microalgae cells is therefore suggested. Nevertheless, the alterations on the FAs profiles observed herein imply that they can be used as metal stress biomarkers, as also suggested for other kinds of stress such as heat (Feijão et al., 2018).

Overall, the increase of total FA content, on a cell basis, observed under CuO ENPs was likely a result of higher cell production of C16:3. The presence of the less functional CuChl *a* supports the need for a higher synthesis of FAs composing thylakoid membranes, to store additional MgChl *a*. Previous studies already reported the importance of chloroplast membrane composition in maintaining PS II stability (Kern and Guskov, 2011). The presence of nanoparticles also affected the omega 6/omega 3 ratio, which was significantly increased due to EPA decrease. Double bond Index only increased for the highest concentration of CuO ENPs ( $10 \mu\text{g L}^{-1}$ ) and is likely a result of the increase in C16:3. The reduction in EPA suggests membrane damage, potentially due to the adhesion of nanoparticles on the plasma membrane or to a higher release of  $\text{Cu}^{2+}$  ions (Zhao et al., 2016), as mentioned before. It is known that the toxicity of CuO ENPs can result from both the exposure to the metal particles themselves and an increased rate in the release of the metal ions (Anyagou et al., 2008; Wang et al., 2012; Baker et al., 2014; Zhao et al., 2016). A full analysis of lipid classes composition

and of the eventual presence of internalized nanoparticles should provide further information on the toxicity mechanisms of CuO engineered nanoparticles.

Further impacts of CuO ENPs were associated with the formation of peroxide radicals via Cu-generated free radicals action found at CuO ENP highest concentration ( $10 \mu\text{g L}^{-1}$ ). Lipid peroxidation is one of the main mechanisms involved in trace metal toxicity through which PUFAs become the main target for free radicals (Rocchetta et al., 2006). The changes in saturated fatty acids (SFA) and PUFA levels caused by copper exposure can be also explained by activation of defense or reparation mechanisms to neutralize cellular damage (Rocchetta et al., 2006). A slightly increasing trend in the activity of some antioxidant enzymes was detected probably due to the relative low Cu concentrations employed in this study, as most studies on antioxidant enzymatic response under copper exposure have been performed using much higher Cu concentrations to evaluate acute stress and lethality (Pinto et al., 2003; Morelli and Scarano, 2004). In the present study, non-lethal concentrations of both Cu in ionic and nanoparticle form were used, allowing cells to maintain viability during the experimental phase, and, at the same time, observe the effects of metal exposure throughout the experiment.

Exposure of *P. tricornutum* cells to both ionic Cu and CuO ENPs resulted in overall increased activity of GR and APX, and a partial increase in CAT, while SOD remained almost unaffected. The more marked increase in GR and APX with CuO ENPs can provide valuable insights on CuO ENP capacity to cause oxidative stress. Copper cations are an important part of the reactive oxygen scavenging system (e.g., CuZnSOD), but they are also able to induce oxidative stress at high concentrations through increased production of ROS (Knauert et al., 2008). Lack of significant induction of CAT and SOD activities suggests minor effects at low Cu concentrations. Studies on *P. tricornutum* already showed that these enzymes play an active role in scavenging of ROS under free copper ions stress (Morelli and Scarano, 2004). Ascorbate is the principal electron donor for APX, and the removal of  $\text{H}_2\text{O}_2$  by APX requires GSH and NADPH (Morelli and Scarano, 2004; Anjum et al., 2016). Fast oxidation of the ascorbate pool can occur under acute stress conditions when high levels of ROS overcome the antioxidant capacity of low molecular weight compounds such as GSH and NADPH (Pinto et al., 2003). It is possible that under Cu exposure conditions, rapid oxidation of the ascorbate pool or depletion of NADPH occurred. The higher activity of GR found in this study also confirms the role of this enzyme in oxidative stress detoxification. Glutathione reductase catalyses the conversion of glutathione disulphide (GSSG) to its reduced form (GSH) in the presence of NADPH (Dringen and Gutterer, 2002; Anjum et al., 2016), and plays a crucial role in maintaining high intracellular [GSH]/[GSSG] ratio. Previous studies already investigated the active detoxification mechanism to avoid trace metal poisoning in plants, algae and fungi (Morelli and Scarano, 2004; Szabó et al., 2008; Anjum et al., 2016), which involves intracellular sequestration of metal ions by GSH and GSH-related peptides named phytochelatin (PCs; Kawakami et al., 2006). Many factors can induce the generation of ROS, and the

modulation detoxification capacity of the organisms can be a winning strategy in chronic exposure to contaminants (Pinto et al., 2003). Overall, ROS toxicity in cells exposed to low concentrations of Cu was not clear, especially regarding the lack of activation of CAT and SOD. Nevertheless, the probable higher bioavailability of  $\text{Cu}^{2+}$  ions associated with CuO ENPs could explain the partial increase in APX and GR activity and clearly differentiated between the effects triggered by ionic Cu and the nanoparticles. Further investigation should clarify the differential activation of the enzymatic pool employed in this study under such non-lethal concentrations.

The alterations found in *P. tricornutum*, particularly those regarding photosynthesis, pigments and FA profiles, triggered by the copper nanoparticles, allow inferring repercussions to the marine food webs and ecosystems. The photosynthetic process was largely compromised by CuO ENPs, which will expectedly have a negative impact on the abundance of phytoplankton assemblages and net primary productivity of marine systems, thereby simultaneously contributing to water deoxygenation. The decline in the omega-3 polyunsaturated FAs, such as EPA, and overall changes in the FA profile at the basis of marine food webs, will expectedly propagate changes to the higher trophic levels. Given that fish natural diet includes high levels of essential LC-PUFA omega-3 (e.g., Ackman, 1989), poor quality phytoplankton in terms of EFAs may reduce the abundance and population dynamics of several species (Gladyshev et al., 2013; Vagner et al., 2015), and, in the long run, compromise humans diet largely relying on fish to obtain these essential compounds. The higher bioavailability of CuO ENPs compared to ionic Cu was demonstrated in our findings and is indicative of higher toxicity risk to marine organisms and ecosystems, even when CuO ENPs are released in relatively low non-lethal concentrations.

## CONCLUSION

The evident changes in photosynthetic performance, the formation of Cu-substituted chlorophyll, the alterations in FA profile observed in the model diatom *P. tricornutum*, suggest that CuO ENPs causes stronger physiological implications compared to their ionic counterparts at similar experimental concentrations. Although our results point toward enhanced  $\text{Cu}^{2+}$  release from CuO ENPs, rather than the internalization of nanoparticles, further research regarding the mechanisms underlying CuO ENPs toxicity is needed to confirm this assumption. The physiology and biochemistry of *P. tricornutum* were very sensitive to CuO ENPs toxicity and provided further insights into diatom-nanoparticle interactions. Several biomarkers were highlighted to efficiently assess the harmful effects of ENPs, including photosynthetic parameters, CuChl *a*, EPA, omega 3/omega 6 ratio, and, to a lesser degree, enzymatic activity (GR, APX). Hence, the proposed biomarkers could be applied to field assessment of the ecological impacts of nanoparticles in marine environments and as tools to support contamination assessment where these emergent metal contaminants are of major concern.

## DATA AVAILABILITY STATEMENT

The datasets generated for this study are available on request to the corresponding author.

## AUTHOR CONTRIBUTIONS

BD conceived and designed the experiments. MF and EF performed the experiments. MF wrote the manuscript. JG performed the SEM analysis and coordinated sample preparation and measurements with the dynamic light scattering system. CP, AM, MC, IC, CG, JM, and PR-S provided technical and editorial assistance. All authors contributed to the article and approved the submitted version.

## FUNDING

The authors would like to thank Fundação para a Ciência e a Tecnologia (FCT) for funding the research via project grants

## REFERENCES

- Abida, H., Dolch, L. J., Mei, C., Villanova, V., Conte, M., Block, M. A., et al. (2015). Membrane glycerolipid remodeling triggered by nitrogen and phosphorus starvation in *Phaeodactylum tricornutum*. *Plant Physiol.* 167, 118–136. doi: 10.1104/pp.114.252395
- Ackman, R. G. (1989). *Marine biogenic lipids, fats and oils*, Florida: CRC Press.
- Allakhverdiev, S. I., Kinoshita, M., Inaba, M., Suzuki, I., and Murata, N. (2001). Unsaturated fatty acids in membrane lipids protect the photosynthetic machinery against salt-induced damage in *Synechococcus*. *Plant Physiol.* 125, 1842–1853. doi: 10.1104/pp.125.4.1842
- Allakhverdiev, S. I., Nishiyama, Y., Suzuki, I., Tasaka, Y., and Murata, N. (1999). Genetic engineering of the unsaturation of fatty acids in membrane lipids alters the tolerance of *Synechocystis* to salt stress. *Proc. Natl. Acad. Sci. U S A.* 96, 5862–5867. doi: 10.1073/pnas.96.10.5862
- Anjum, N. A., Duarte, B., Caçador, I., Sleimi, N., Duarte, A. C., and Pereira, E. (2016). Biophysical and Biochemical Markers of Metal/Metalloid-Impacts in Salt Marsh Halophytes and Their Implications. *Front. Environ. Sci.* 4:1–13. doi: 10.3389/fenvs.2016.00024
- Ansari, T. M., Marr, I. L., and Tariq, N. (2004). Heavy metals in marine pollution perspective—a mini review. *J. Appl. Sci.* 4, 1–20. doi: 10.3923/jas.2004.1.20
- Anyagou, K. C., Fedorov, A. V., and Neckers, D. C. (2008). Synthesis, characterization, and antifouling potential of functionalized copper nanoparticles. *Langmuir* 24, 4340–4346. doi: 10.1021/la800102f
- Arao, T., Kawaguchi, A., and Yamada, M. (1987). Positional distribution of fatty acids in lipids of the marine diatom *Phaeodactylum tricornutum*. *Phytochemistry* 26, 2573–2576. doi: 10.1016/S0031-9422(00)83880-7
- Arts, M. T., Ackman, R. G., and Holub, B. J. (2001). "Essential fatty acids" in aquatic ecosystems: a crucial link between diet and human health and evolution. *Can. J. Fisher. Aqua. Sci.* 58, 122–137. doi: 10.1139/f00-224
- Aruoja, V., Dubourguier, H. C., Kasemets, K., and Kahru, A. (2009). Toxicity of nanoparticles of CuO, ZnO and TiO<sub>2</sub> to microalgae *Pseudokirchneriella subcapitata*. *Sci. Total Environ.* 407, 1461–1468. doi: 10.1016/j.scitotenv.2008.10.053
- Baker, T. J., Tyler, C. R., and Galloway, T. S. (2014). Impacts of metal and metal oxide nanoparticles on marine organisms. *Environ. Pollut.* 186, 257–271. doi: 10.1016/j.envpol.2013.11.014
- Cabrita, M. T., Duarte, B., Gameiro, C., Godinho, R. M., and Caçador, I. (2018). Photochemical features and trace element substituted chlorophylls as early detection biomarkers of metal exposure in the model diatom *Phaeodactylum tricornutum*. *Ecol. Indicat.* 95, 1038–1052. doi: 10.1016/j.ecolind.2017.07.057
- PTDC/CTA-AMB/30056/2017 (OPTOX), UIDB/04292/2020, and UID/MULTI/04046/2013. BD and VF were supported by investigation contracts (CEECIND/00511/2017 and DL57/2016/CP1479/CT0024). PR-S was supported by FCT through a postdoctoral grant (SFRH/BPD/95784/2013). JG was supported by co-funding through the NanoTRAINforGrowth II Program (project 2000032) by the European Commission through the Horizon 2020 Marie Skłodowska-Curie COFUND Program (2015), and by the International Iberian Nanotechnology Laboratory.

## SUPPLEMENTARY MATERIAL

The Supplementary Material for this article can be found online at: <https://www.frontiersin.org/articles/10.3389/fmars.2020.539827/full#supplementary-material>

**Supplementary Figure 1** | Copper ENPs SEM imaging at 35,000x (A), 50,000x (B), 80,000x (C), and 150,000 (d) magnification and X-ray fluorescence spectra elemental composition (D).

- Cabrita, M. T., Gameiro, C., Utkin, A. B., Duarte, B., Caçador, I., and Cartaxana, P. (2016). Photosynthetic pigment laser-induced fluorescence indicators for the detection of changes associated with trace element stress in the diatom model species *Phaeodactylum tricornutum*. *Environ. Monit. Assess.* 188:285. doi: 10.1007/s10661-016-5293-4
- Cabrita, M. T., Raimundo, J., Pereira, P., and Vale, C. (2013). Optimizing alginate beads for the immobilisation of *Phaeodactylum tricornutum* in estuarine waters. *Mar. Environ. Res.* 8, 37–43. doi: 10.1016/j.marenvres.2013.03.002
- Cabrita, M. T., Raimundo, J., Pereira, P., and Vale, C. (2014). Immobilised *Phaeodactylum tricornutum* as biomonitor of trace element availability in the water column during dredging. *Environ. Sci. Pollut. Res. Int.* 21, 3572–3581. doi: 10.1007/s11356-013-2362-x
- Chen, C., Zhang, J., Ma, P., Jin, K., Li, L., and Luan, J. (2012). Spatial-temporal distribution of phytoplankton and safety assessment of water quality in Xikeng reservoir. *Hydroecology* 33, 32–38.
- Cid, A., Herrero, C., Torres, E., and Abalde, J. (1995). Copper toxicity on the marine microalga *Phaeodactylum tricornutum*: effects on photosynthesis and related parameters. *Aquat. Toxicol.* 31, 165–174. doi: 10.1016/0166-445X(94)00071-W
- Din, M. I., and Rehan, R. (2017). Synthesis, Characterization, and Applications of Copper Nanoparticles. *Anal. Lett.* 50, 50–62. doi: 10.1080/00032719.2016.1172081
- Dolch, L. J., and Maréchal, E. (2015). Inventory of fatty acid desaturases in the pennate diatom *Phaeodactylum tricornutum*. *Mar. Drugs* 13, 1317–1339. doi: 10.3390/md13031317
- Dringen, R., and Gutterer, J. M. (2002). Glutathione reductase from bovine brain. *Methods Enzymol.* 348, 281–288. doi: 10.1016/S0076-6879(02)48646-6
- Duarte, B., Cabrita, M. T., Gameiro, C., Matos, A. R., Godinho, R., Marques, J. C., et al. (2017). Disentangling the photochemical salinity tolerance in *Aster tripolium* L.: connecting biophysical traits with changes in fatty acid composition. *Plant Biol.* 19, 239–248. doi: 10.1111/plb.12517
- Duarte, B., Caetano, M., Almeida, P. R. R., Vale, C., and Caçador, I. (2010). Accumulation and biological cycling of heavy metal in four salt marsh species, from Tagus estuary (Portugal). *Environ. Pollut.* 158, 1661–1668. doi: 10.1016/j.envpol.2009.12.004
- Duarte, B., Marques, J. C., and Caçador, I. (2016). Ecophysiological response of native and invasive *Spartina* species to extreme temperature events in Mediterranean marshes. *Biol. Invas.* 18, 2189–2205. doi: 10.1007/s10530-015-0958-4
- Duarte, B., Prata, D., Matos, A., Rita, Cabrita, M., Teresa, et al. (2019). Ecotoxicity of the lipid-lowering drug bezafibrate on the bioenergetics and lipid metabolism

- of the diatom *Phaeodactylum tricornutum*. *Sci. Total Environ.* 650, 2085–2094. doi: 10.1016/j.scitotenv.2018.09.354
- Duarte, B., Silva, G., Costa, J. L., Medeiros, J., Paulo, Azeda, C., et al. (2014). Heavy metal distribution and partitioning in the vicinity of the discharge areas of Lisbon drainage basins (Tagus Estuary, Portugal). *J. Sea Res.* 93, 101–111. doi: 10.1016/j.seares.2014.01.003
- Dunstan, G. A., Volkman, J. K., Barrett, S. M., Leroi, J. M., and Jeffrey, S. W. (1993). Essential polyunsaturated fatty acids from 14 species of diatom (Bacillariophyceae). *Phytochemistry* 35, 155–161. doi: 10.1016/S0031-9422(00)90525-9
- Fan, K.-W., Jiang, Y., Faan, Y.-W., and Chen, F. (2007). Lipid characterization of mangrove thraustochytrid–Schizochytrium mangrovei. *J. Agric. Food Chem.* 55, 2906–2910. doi: 10.1021/jf070058y
- Feijão, E., Gameiro, C., Franzitta, M., Duarte, B., Caçador, I., Cabrita, M., et al. (2018). Heat wave impacts on the model diatom *Phaeodactylum tricornutum*: Searching for photochemical and fatty acid biomarkers of thermal stress. *Ecol. Indic.* 95, 1026–1037. doi: 10.1016/j.ecolind.2017.07.058
- Fernandes, J. C., and Henriques, F. S. (1991). Biochemical, Physiological, and Structural Effects of Excess Copper in Plants. *Bot. Rev.* 57, 246–273. doi: 10.1007/bf02858564
- Filimonova, V., Gonçalves, F., Marques, J. C., De Troch, M., and Gonçalves, A. M. M. (2016). Fatty acid profiling as bioindicator of chemical stress in marine organisms: A review. *Ecol. Indic.* 67, 657–672. doi: 10.1016/j.ecolind.2016.03.044
- Foyer, C. H., and Halliwell, B. (1976). The presence of glutathione and glutathione reductase in chloroplasts: A proposed role in ascorbic acid metabolism. *Planta* 133, 21–25. doi: 10.1007/BF00386001
- Gladyshev, M. I., Sushchik, N. N., and Makhutova, O. N. (2013). Production of EPA and DHA in aquatic ecosystems and their transfer to the land. *Prostagl. Other Lipid Mediat.* 107, 117–126. doi: 10.1016/j.prostaglandins.2013.03.002
- Guillard, R. R. L., and Ryther, J. H. (1962). Studies of Marine Planktonic Diatoms: I. *Cyclotella* Nana Hustedt, and *Detonula* Confervacea (Cleve) Gran. *Can. J. Microbiol.* 8, 229–239. doi: 10.1139/m62-029
- Heath, R. L., and Packer, L. (1968). Photoperoxidation in isolated chloroplasts. *Arch. Biochem. Biophys.* 125, 189–198. doi: 10.1016/0003-9861(68)90654-1
- Hook, S. E., Osborn, H. L., Gissi, F., Moncuquet, P., Twine, N. A., Wilkins, M. R., et al. (2014). RNA-Seq analysis of the toxicant-induced transcriptome of the marine diatom, *Ceratoneis closterium*. *Mar. Genom.* 16, 45–53. doi: 10.1016/j.margen.2013.12.004
- Horie, M., Fujita, K., Kato, H., Endoh, S., Nishio, K., Komaba, L. K., et al. (2012). Association of the physical and chemical properties and the cytotoxicity of metal oxide nanoparticles: metal ion release, adsorption ability and specific surface area. *Metallomics* 4, 350–360. doi: 10.1039/c2mt20016c
- Kawakami, S. K., Gledhill, M., and Achterberg, E. P. (2006). Production of phytochelatin and glutathione by marine phytoplankton in response to metal stress. *J. Phycol.* 42, 975–989. doi: 10.1111/j.1529-8817.2006.00265.x
- Kern, J., and Guskov, A. (2011). Lipids in photosystem II: Multifunctional cofactors. *J. Photochem. Photobiol. B Biol.* 104, 19–34. doi: 10.1016/j.jphotobiol.2011.02.025
- Klaine, S. J., Alvarez, P. J. J., Batley, G. E., Fernandes, T. F., Handy, R. D., Lyon, D. Y., et al. (2008). Nanomaterials in the Environment: Behavior, Fate, Bioavailability, and Effects. *Environ. Toxicol. Chem.* 27, 1825–1851. doi: 10.1897/08-090.1
- Knauer, S., Escher, B., Singer, H., Hollender, J., and Knauer, K. (2008). Mixture toxicity of three photosystem II inhibitors (atrazine, isoproturon, and diuron) toward photosynthesis of freshwater phytoplankton studied in outdoor mesocosms. *Environ. Sci. Technol.* 42, 6424–6430. doi: 10.1021/es072037q
- Kruse, O., Hankamer, B., Konczak, C., Gerle, C., Morris, E., Radunz, A., et al. (2000). Phosphatidylglycerol is involved in the dimerization of photosystem II. *J. Biol. Chem.* 275, 6509–6514. doi: 10.1074/jbc.275.9.6509
- Kumar, K. S., Dahms, H. U., Lee, J. S., Kim, H. C., Lee, W. C., and Shin, K. H. (2014). Algal photosynthetic responses to toxic metals and herbicides assessed by chlorophyll a fluorescence. *Ecotoxicol. Environ. Saf.* 104, 51–71. doi: 10.1016/j.jecoenv.2014.01.042
- Küpper, H., and Spiller, M. (1998). In Situ Detection of Heavy Metal Substituted Chlorophylls in Water Plants. *Photosynth. Res.* 58, 123–133. doi: 10.1023/A:1006132608181
- Küpper, H., Seibert, S., and Parameswaran, A. (2007). Fast, sensitive, and inexpensive alternative to analytical pigment HPLC: quantification of chlorophylls and carotenoids in crude extracts by fitting with Gauss peak spectra. *Analyt. Chem.* 79, 7611–7627. doi: 10.1021/ac070236m
- Küpper, H., Šetlik, I., Spiller, M., Küpper, F. C., and Prášil, O. (2002). Heavy metal-induced inhibition of photosynthesis: Targets of in vivo heavy metal chlorophyll formation. *J. Phycol.* 38, 429–441. doi: 10.1046/j.1529-8817.2002.t01-1-01148.x
- Li, Y.-F., Gao, Y., Chai, Z., and Chen, C. (2014). Nanometallics: an emerging field studying the biological effects of metal-related nanomaterials. *Metallomics* 6, 220–232. doi: 10.1039/c3mt00316g
- Marklund, S., and Marklund, G. (1974). Involvement of the Superoxide Anion Radical in the Autoxidation of Pyrogallol and a Convenient Assay for Superoxide Dismutase. *Eur. J. Biochem.* 47, 469–474. doi: 10.1111/j.1432-1033.1974.tb03714.x
- Mohanty, N., Vass, I., and Demeter, S. (1989). Copper Toxicity Affects Photosystem II Electron Transport at the Secondary Quinone Acceptor, Q(B). *Plant Physiol.* 90, 175–179. doi: 10.1104/pp.90.1.175
- Morelli, E., and Scarano, G. (2004). Copper-induced changes of non-protein thiols and antioxidant enzymes in the marine microalga *Phaeodactylum tricornutum*. *Plant Sci.* 167, 289–296. doi: 10.1016/j.plantsci.2004.04.001
- Nowack, B., and Bucheli, T. D. (2007). Occurrence, behavior and effects of nanoparticles in the environment. *Environ. Pollut.* 150, 5–22. doi: 10.1016/j.envpol.2007.06.006
- Oberdörster, G., Oberdörster, E., and Oberdörster, J. (2005). Nanotoxicology: An emerging discipline evolving from studies of ultrafine particles. *Environ. Health Perspect.* 113, 823–839. doi: 10.1289/ehp.7339
- OECD (2011). OECD Guidelines for the testing of Chemicals. Freshwater Alga and Cyanobacteria, Growth Inhibition Test. *Organ. Econ. Coop. Dev.* 2011, 1–25. doi: 10.1787/9789264203785-en
- Pan, K., and Wang, W.-X. (2012). Trace metal contamination in estuarine and coastal environments in China. *Sci. Total Environ.* 42, 3–16. doi: 10.1016/j.scitotenv.2011.03.013
- Parrish, C. C. (2009). *Essential fatty acids in aquatic food webs. In Lipids in aquatic ecosystems.* New York, NY: Springer, 309–326.
- Patsikka, E., Aro, E., and Tyystjärvi, E. (1998). Increase in the quantum yield of photoinhibition contributes to copper toxicity in vivo. *Plant Physiol.* 117, 619–627. doi: 10.1104/pp.117.2.619
- Pinto, E., Sigaud-Kutner, T. C. S., Leitao, M. A. S., Okamoto, O. K., Morse, D., and Calepicolo, P. (2003). Review - Heavy metal-induced oxidative stress in algae. *J. Phycol.* 39, 1008–1018. doi: 10.1111/j.0022-3646.2003.02-193.x
- Popko, J., Herrfurth, C., Feussner, K., Ischebeck, T., Iven, T., Haslam, R., et al. (2016). Metabolome Analysis Reveals Betaine Lipids as Major Source for Triglyceride Formation, and the Accumulation of Sedoheptulose during Nitrogen-Starvation of *Phaeodactylum tricornutum*. *PLoS One* 11:e0164673. doi: 10.1371/journal.pone.0164673
- Prosi, F. (1981). *Heavy metals in aquatic organisms. In Metal pollution in the aquatic environment.* Berlin: Springer, 271–323.
- Remmers, I. M., Martens, D. E., Wijffels, R. H., and Lamers, P. P. (2017). Dynamics of triacylglycerol and EPA production in *Phaeodactylum tricornutum* under nitrogen starvation at different light intensities. *PLoS One* 12:e0175630. doi: 10.1371/journal.pone.0175630
- Research And Markets.com. (2018). *Metal Nanoparticles Market by metal (Platinum, Gold, Silver, Iron, Titanium, Copper, Nickel), End-use industry (Pharmaceutical & healthcare, Electrical & electronics, Catalyst, Personal care & cosmetics), and Region - Global Forecast to 2022.* California: Business Wire.
- Rip, A., Misa, T. J., and Schot, J. (eds) (1995). *Managing technology in society.* London: Pinter Publishers.
- Rocchetta, I., Mazzuca, M., Conforti, V., Ruiz, L., Balzaretto, V., and De Molina, M. D. C. R. (2006). Effect of chromium on the fatty acid composition of two strains of *Euglena gracilis*. *Environ. Pollut.* 141, 353–358. doi: 10.1016/j.envpol.2005.08.035
- Royal Commission on Environmental Pollution. (2008). *Novel materials in the environment: the case of nanotechnology.* London: The Stationery Office.
- Saito, H., and Aono, H. (2014). Characteristics of lipid and fatty acid of marine gastropod *Turbo cornutus*: High levels of arachidonic and n-3 docosapentaenoic acid. *Food Chem.* 145, 135–144. doi: 10.1016/j.foodchem.2013.08.011

- Santos-Ballardo, D. U., Rossi, S., Hernández, V., Gómez, R. V., del Carmen, Rendón-Unceta, M., et al. (2015). A simple spectrophotometric method for biomass measurement of important microalgae species in aquaculture. *Aquaculture* 448, 87–92. doi: 10.1016/j.aquaculture.2015.05.044
- Sharma, K. K., Schuhmann, H., and Schenk, P. M. (2012). High lipid induction in microalgae for biodiesel production. *Energies* 5, 1532–1553. doi: 10.3390/en5051532
- Shen, P. L., Wang, H. T., Pan, Y. F., Meng, Y. Y., Wu, P. C., and Xue, S. (2016). Identification of Characteristic Fatty Acids to Quantify Triacylglycerols in Microalgae. *Front. Plant Sci.* 7:162. doi: 10.3389/fpls.2016.00162
- Sunda, W. G. (1989). Trace metal interactions with marine phytoplankton. *Biol. Oceanogr.* 6, 411–442. doi: 10.1080/01965581.1988.10749543
- Szabó, M., Lepetit, B., Goss, R., Wilhelm, C., Mustárdy, L., and Garab, G. (2008). Structurally flexible macro-organization of the pigment-protein complexes of the diatom *Phaeodactylum tricornutum*. *Photosynth. Res.* 95, 237–245. doi: 10.1007/s11120-007-9252-3
- Teranishi, Y., Tanaka, A., Osumi, M., and Fukui, S. (1974). Catalase activities of hydrocarbon-utilizing candida yeasts. *Agric. Biol. Chem.* 38, 1213–1220. doi: 10.1080/00021369.1974.10861301
- Tiryakioglu, M., Eker, S., Ozkutlu, F., Husted, S., and Cakmak, I. (2006). Antioxidant defense system and cadmium uptake in barley genotypes differing in cadmium tolerance. *J. Trace Elem. Med. Biol.* 20, 181–189. doi: 10.1016/j.jtemb.2005.12.004
- Twining, B. S., and Baines, S. B. (2013). The trace metal composition of marine phytoplankton. *Annu. Rev. Mar. Sci.* 5, 191–215. doi: 10.1146/annurev-marine-121211-172322
- UNEP (2006). *Marine and coastal ecosystems and human well-being: A synthesis report based on the findings of the Millennium Ecosystem Assessment*. Kenya: UNEP.
- Vagner, M., Lacoue-Labarthe, T., Zambonino Infante, J. L., Mazurais, D., Dubillot, E., Le Delliou, H., et al. (2015). Depletion of Essential Fatty Acids in the Food Source Affects Aerobic Capacities of the Golden Grey Mullet *Liza aurata* in a Warming Seawater Context. *PLoS One* 10:e0126489. doi: 10.1371/journal.pone.0126489
- Wang, Z., Li, N., Zhao, J., White, J. C., Qu, P., and Xing, B. (2012). CuO nanoparticle interaction with human epithelial cells: Cellular uptake, location, export, and genotoxicity. *Chem. Res. Toxicol.* 25, 1512–1521. doi: 10.1021/tx3002093
- Wei, Y., Zhu, N., Lavoie, M., Wang, J., Qian, H., and Fu, Z. (2014). Copper toxicity to *Phaeodactylum tricornutum*: A survey of the sensitivity of various toxicity endpoints at the physiological, biochemical, molecular and structural levels. *BioMetals* 27, 527–537. doi: 10.1007/s10534-014-9727-6
- Yang, Y. H., Du, L., Hosokawa, M., Miyashita, K., Kokubun, Y., Arai, H., et al. (2017). Fatty Acid and Lipid Class Composition of the Microalga *Phaeodactylum tricornutum*. *J. Oleo Sci.* 66, 363–368. doi: 10.5650/jos.ess.16205
- Zhang, C., Chen, X., Tan, L., and Wang, J. (2018). Combined toxicities of copper nanoparticles with carbon nanotubes on marine microalgae *Skeletonema costatum*. *Environ. Sci. Pollut. Res.* 25, 13127–13133. doi: 10.1007/s11356-018-1580-7
- Zhao, J., Cao, X., Liu, X., Wang, Z., Zhang, C., White, J. C., et al. (2016). Interactions of CuO nanoparticles with the algae *Chlorella pyrenoidosa*: adhesion, uptake, and toxicity. *Nanotoxicology* 10, 1297–1305. doi: 10.1080/17435390.2016.1206149
- Zhu, X. G., Govindjee, Baker, N. R., DeSturler, E., Ort, D. R., and Long, S. P. (2005). Chlorophyll a fluorescence induction kinetics in leaves predicted from a model describing each discrete step of excitation energy and electron transfer associated with Photosystem II. *Planta* 223, 114–133. doi: 10.1007/s00425-005-0064-4
- Zhu, Y., Xu, J., Lu, T., Zhang, M., Ke, M., Fu, Z., et al. (2017). A comparison of the effects of copper nanoparticles and copper sulfate on *Phaeodactylum tricornutum* physiology and transcription. *Environ. Toxicol. Pharmacol.* 56, 43–49. doi: 10.1016/j.etap.2017.08.029

**Conflict of Interest:** The authors declare that the research was conducted in the absence of any commercial or financial relationships that could be construed as a potential conflict of interest.

Copyright © 2020 Franzitta, Feijão, Cabrita, Gameiro, Matos, Marques, Goessling, Reis-Santos, Fonseca, Pretti, Caçador and Duarte. This is an open-access article distributed under the terms of the Creative Commons Attribution License (CC BY). The use, distribution or reproduction in other forums is permitted, provided the original author(s) and the copyright owner(s) are credited and that the original publication in this journal is cited, in accordance with accepted academic practice. No use, distribution or reproduction is permitted which does not comply with these terms.